Computers and Structures 298 (2024) 107350

Contents lists available at ScienceDirect

Computers and Structures

journal homepage: www.elsevier.com/locate/compstruc

Towards optimal use of the explicit β_1/β_2-Bathe time integration method for linear and nonlinear dynamics

Mohammad Mahdi Malakiyeh [a], Zahra Anjomshoae [a], Saeed Shojaee [a], Saleh Hamzehei-Javaran [a], Klaus-Jürgen Bathe [b,*]

[a] Department of Civil Engineering, Shahid Bahonar University of Kerman, Kerman, Iran
[b] Massachusetts Institute of Technology, Cambridge, MA 02139, United States

ARTICLE INFO

Keywords:
Direct time integration
Explicit β_1/β_2-Bathe method
Linear and nonlinear dynamics
Effect of physical damping
Stability and solution accuracy
Numerical damping

ABSTRACT

In an earlier publication, we proposed a new explicit time integration scheme, the β_1/β_2-Bathe method, which is simple in its formulation and showed remarkable accuracy in the solution of problems [1]. A particular strength of the method is that it can directly be used as a first-order or second-order scheme by a change of the values of β_1 and β_2. While good results are obtained with reasonable values of β_1 and β_2, for excellent accuracy better values of the parameters need to be chosen. We propose in this paper values of β_1 and β_2 for the first-order scheme, best used in wave propagation analyses, and separate values for the second-order scheme, best used in analyses of structural vibrations. In each case, one set of values of (β_1, β_2) is given and to possibly improve the results only one of the parameters needs to be changed, that is, β_1 for wave propagations and β_2 for structural vibrations, making the scheme a one-parameter method. Another strength of the procedure is that physical damping can directly be included in the solution, the effect of which on the stability and accuracy of the solutions we analyze in the paper. The use of the solution scheme in nonlinear analysis is, as we show in the paper, a simple extension from linear analysis. Finally, we give various solutions using the explicit β_1/β_2-Bathe method in linear and nonlinear analyses to illustrate the performance of the method with the given recommendations for its use.

1. Introduction

When addressing the solution of dynamic problems in practical applications, numerical methods play an essential role in solving the governing equations. Among the available numerical methods, direct time integration methods are widely used, and indeed play a pivotal role in solving time-dependent finite element equations. They can be categorized into two main groups: implicit and explicit methods. Implicit methods can be conditionally or unconditionally stable, whereas explicit schemes are inherently conditionally stable [2]. Extensive research efforts have been dedicated to increasing the effectiveness of direct time integration methods because even seemingly small increases in effectiveness can be very important in engineering practice and computational science. These efforts have led to the proposal of various explicit and implicit methods, see for example [1–29].

When employing diagonal mass and damping matrices, explicit methods typically require less computational effort within each time step than implicit schemes. On the other hand, using an unconditionally stable implicit method frequently allows the use of much larger time steps which can result in a lower total analysis cost. The choice of which method then to use for the most effective solution can be difficult. However, there are instances when an explicit method should be more efficient, notably when the applied loads or the calculation of the response necessitate the utilization of a small time step. In addition, an explicit scheme may also be more effective in the solution of a nonlinear problem [2–4].

It is well-known that the presence of numerical damping in a direct time integration solution scheme can be important. In order to attain good accuracy in a response prediction, it is imperative for direct time integration methods to impose, automatically, some numerical damping in the solution. The numerical damping through the solution scheme should prevent spurious response due to high non-physical frequencies in the mesh. The difficulty, however, is that the numerical damping should be just enough to rapidly damp out the spurious frequencies with the largest time step possible, while giving good accuracy in the response prediction [2,7,10,12,13,14].

* Corresponding author.
E-mail address: kjb@mit.edu (K.J. Bathe).

https://doi.org/10.1016/j.compstruc.2024.107350
Received 29 January 2024; Accepted 17 March 2024
Available online 24 April 2024

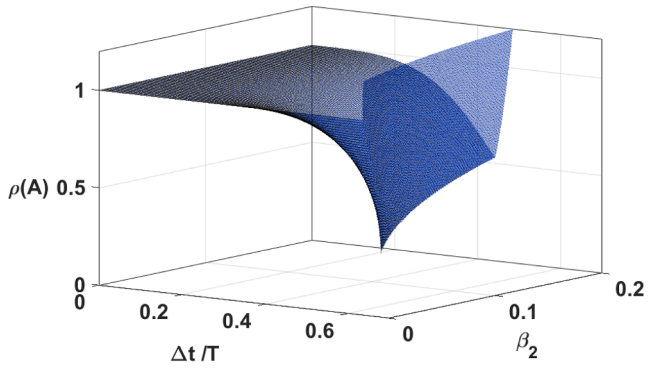

(a) Three-dimensional plot (3D plot)

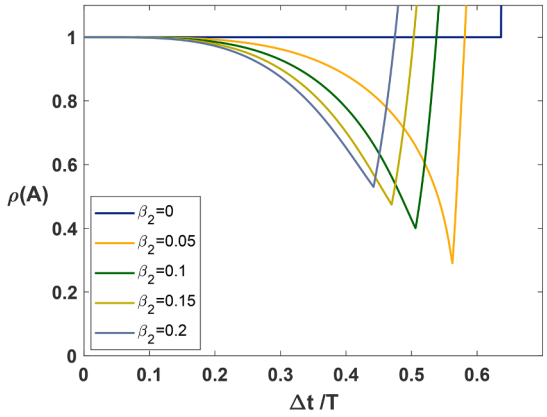

(b) Two-dimensional plot (2D plot)

Fig. 1. Spectral radius of the explicit β_1/β_2-Bathe method for $\beta_1 = 0.5$ (second-order accuracy).

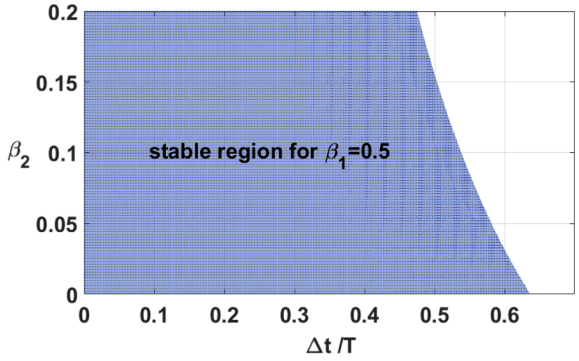

Fig. 2. Stable region of the explicit β_1/β_2-Bathe method for $\beta_1 = 0.5$ (second-order accuracy).

Recently, we introduced the explicit β_1/β_2-Bathe method [1] which uses two sub-steps, like employed in all Bathe direct time integration schemes. An important quality is that the scheme uses the equilibrium equations at the end of each sub-step to advance the solution to that time. In the computations we use, for each sub-step, first a Taylor series to predict the velocities and displacements in order to solve for the unknown accelerations. Subsequently, we update these predictions by adding correction terms involving the just calculated accelerations. The correction term for the velocities uses the parameter β_1 and the correction term for the displacements uses β_2.

In this paper, we further study the explicit β_1/β_2-Bathe method to identify optimal values of the parameters β_1 and β_2 to use in solutions. These values are more effective to use than those given in Ref. [1]. We

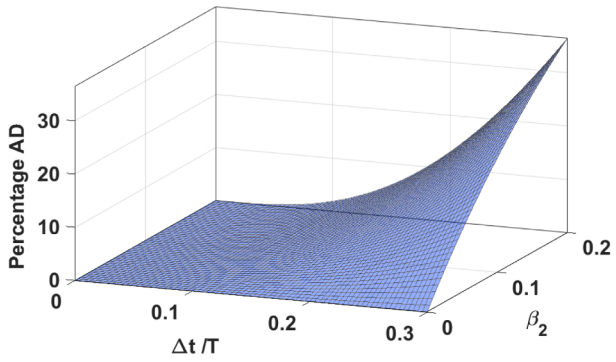

(a) 3D plot

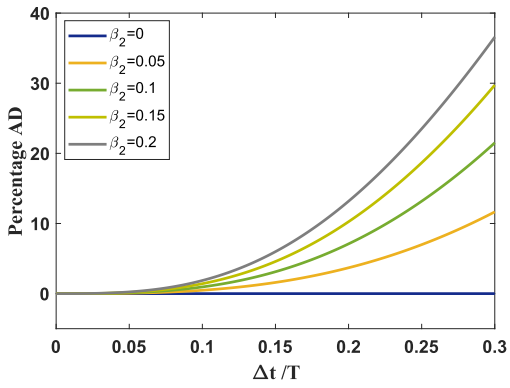

(b) 2D plot

Fig. 3. Amplitude decay of the explicit β_1/β_2-Bathe method for $\beta_1 = 0.5$ (second-order accuracy).

give the spectral radii, amplitude decays and period elongations when the recommended values of β_1 and β_2 are used and also identify the critical time step when physical damping is included in the solution. In addition, we give the equations to use for nonlinear analysis and present some illustrative solutions of linear and nonlinear problems.

2. The fundamental equations

In this section, we present the fundamental equations of the explicit β_1/β_2-Bathe time integration method for linear and nonlinear dynamics.

2.1. Linear dynamics

In the explicit β_1/β_2-Bathe method, like in all Bathe family time integration methods, we use two sub-steps of size $\gamma\Delta t$ and $(1-\gamma)\Delta t$. In linear dynamics, for the first sub-step, we use the following equations,

$$\mathbf{M}\,{}^{t+\gamma\Delta t}\ddot{\mathbf{U}} = {}^{t+\gamma\Delta t}\mathbf{R} - \mathbf{C}\Big[{}^{t}\dot{\mathbf{U}} + (\gamma\Delta t)\,{}^{t}\ddot{\mathbf{U}}\Big] - \mathbf{K}\Big[{}^{t}\mathbf{U} + (\gamma\Delta t)\,{}^{t}\dot{\mathbf{U}} + (0.5)(\gamma\Delta t)^2\,{}^{t}\ddot{\mathbf{U}}\Big] \tag{1}$$

$${}^{t+\gamma\Delta t}\dot{\mathbf{U}} = {}^{t}\dot{\mathbf{U}} + (\gamma\Delta t)\,{}^{t}\ddot{\mathbf{U}} + \beta_1(\gamma\Delta t)\Big({}^{t+\gamma\Delta t}\ddot{\mathbf{U}} - {}^{t}\ddot{\mathbf{U}}\Big) \tag{2}$$

$${}^{t+\gamma\Delta t}\mathbf{U} = {}^{t}\mathbf{U} + (\gamma\Delta t)\,{}^{t}\dot{\mathbf{U}} + (0.5)(\gamma\Delta t)^2\,{}^{t}\ddot{\mathbf{U}} + \beta_2(\gamma\Delta t)^2\Big({}^{t+\gamma\Delta t}\ddot{\mathbf{U}} - {}^{t}\ddot{\mathbf{U}}\Big) \tag{3}$$

We employ Eq. (1) to obtain the acceleration response at $t+\gamma\Delta t$, and then use Eqs. (2) and (3), respectively, to obtain the vectors of velocity and displacement at $t+\gamma\Delta t$. In these equations and below, we use our usual notation for the mass, damping, and stiffness matrices, the

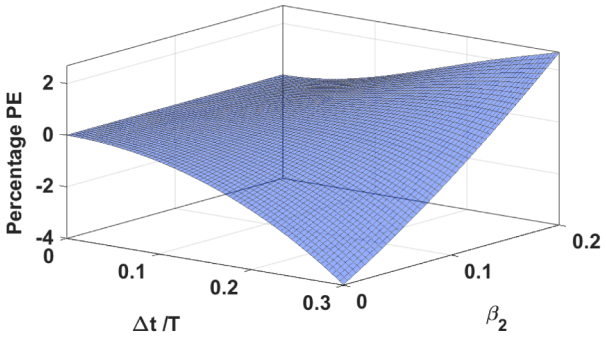

(a) 3D plot

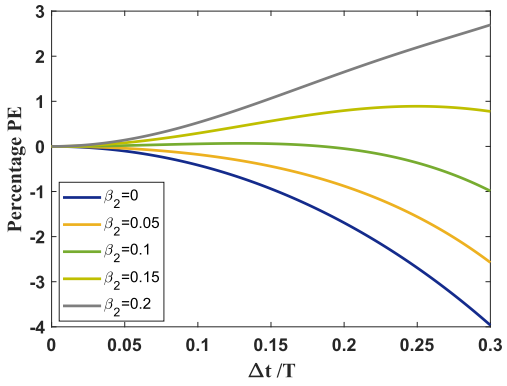

(b) 2D plot

Fig. 4. Period elongation of the explicit β_1/β_2-Bathe method for $\beta_1 = 0.5$ (second-order accuracy).

acceleration, velocity, and displacement vectors, and for all variables in the time stepping and stability and accuracy analyses [1,2].

For the second sub-step, we use the following equations,

$$\begin{aligned}\mathbf{M}\,{}^{t+\Delta t}\ddot{\mathbf{U}} = {}^{t+\Delta t}\mathbf{R} - \mathbf{C}\left[{}^{t+\gamma\Delta t}\dot{\mathbf{U}} + (1-\gamma)(\Delta t)\,{}^{t+\gamma\Delta t}\ddot{\mathbf{U}}\right]\\ -\mathbf{K}\left[{}^{t+\gamma\Delta t}\mathbf{U} + (1-\gamma)(\Delta t)\,{}^{t+\gamma\Delta t}\dot{\mathbf{U}} + (0.5)(1-\gamma)^2(\Delta t)^2\,{}^{t+\gamma\Delta t}\ddot{\mathbf{U}}\right]\end{aligned} \tag{4}$$

$${}^{t+\Delta t}\dot{\mathbf{U}} = {}^{t+\gamma\Delta t}\dot{\mathbf{U}} + (1-\gamma)(\Delta t)\,{}^{t+\gamma\Delta t}\ddot{\mathbf{U}} + \beta_1(1-\gamma)(\Delta t)\left({}^{t+\Delta t}\ddot{\mathbf{U}} - {}^{t+\gamma\Delta t}\ddot{\mathbf{U}}\right) \tag{5}$$

$$\begin{aligned}{}^{t+\Delta t}\mathbf{U} = {}^{t+\gamma\Delta t}\mathbf{U} + (1-\gamma)(\Delta t)\,{}^{t+\gamma\Delta t}\dot{\mathbf{U}} + (0.5)(1-\gamma)^2(\Delta t)^2\,{}^{t+\gamma\Delta t}\ddot{\mathbf{U}}\\ +\beta_2(1-\gamma)^2(\Delta t)^2\left({}^{t+\Delta t}\ddot{\mathbf{U}} - {}^{t+\gamma\Delta t}\ddot{\mathbf{U}}\right)\end{aligned} \tag{6}$$

Now we use Eq. (4) to obtain the acceleration response at $t + \Delta t$, and then use Eqs. (5) and (6), respectively, to obtain the velocity and displacement vectors at $t+\Delta t$.

2.2. Nonlinear dynamics

In nonlinear dynamics, Eq. (1) to obtain the nodal accelerations at $t+\gamma\Delta t$ is changed to

$$\mathbf{M}\,{}^{t+\gamma\Delta t}\ddot{\mathbf{U}} = {}^{t+\gamma\Delta t}\mathbf{R} - {}^{t+\gamma\Delta t}\widetilde{\mathbf{F}} - \mathbf{C}\left[{}^{t}\dot{\mathbf{U}} + (\gamma\Delta t)\,{}^{t}\ddot{\mathbf{U}}\right] \tag{7}$$

where ${}^{t+\gamma\Delta t}\widetilde{\mathbf{F}}$ are the nodal forces corresponding to the element stresses at the displacements ${}^{t+\gamma\Delta t}\mathbf{U}$ with

$${}^{t+\gamma\Delta t}\mathbf{U} = {}^{t}\mathbf{U} + (\gamma\Delta t)\,{}^{t}\dot{\mathbf{U}} + (0.5)(\gamma\Delta t)^2\,{}^{t}\ddot{\mathbf{U}} \tag{8}$$

Then we proceed as in linear dynamics, that is, Eqs. (2) and (3) give

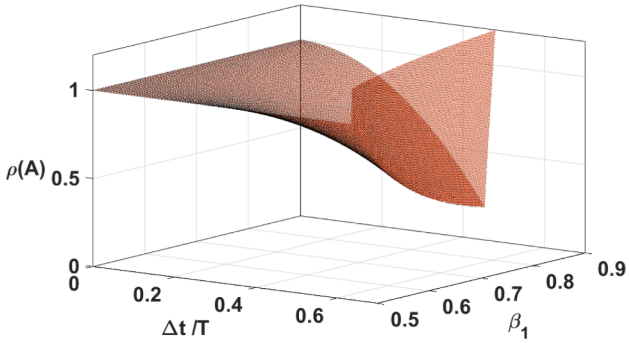

(a) 3D plot

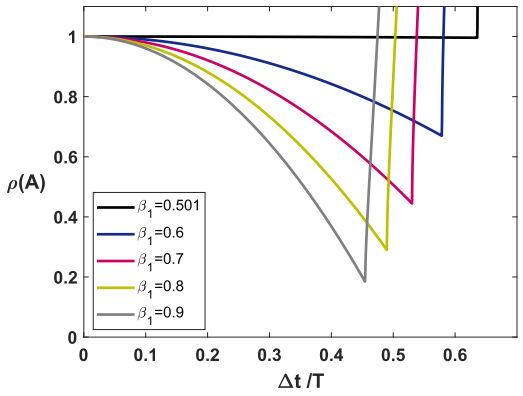

(b) 2D plot

Fig. 5. Spectral radius of the explicit β_1/β_2-Bathe method for $\beta_2 = 0$ (first-order accuracy).

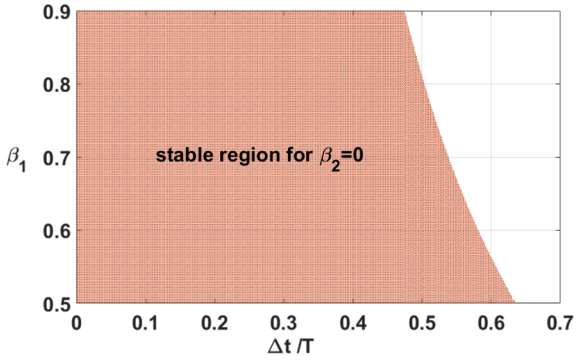

Fig. 6. Stable region of the explicit β_1/β_2-Bathe method for $\beta_2 = 0$ (first-order accuracy).

the velocity and displacement vectors at $t + \gamma\Delta t$.

For the second sub-step, Eq. (4) is modified to

$$\mathbf{M}\,{}^{t+\Delta t}\ddot{\mathbf{U}} = {}^{t+\Delta t}\mathbf{R} - {}^{t+\Delta t}\widetilde{\mathbf{F}} - \mathbf{C}\left[{}^{t+\gamma\Delta t}\dot{\mathbf{U}} + (1-\gamma)(\Delta t)\,{}^{t+\gamma\Delta t}\ddot{\mathbf{U}}\right] \tag{9}$$

where ${}^{t+\Delta t}\widetilde{\mathbf{F}}$ are the nodal forces at time $t+\Delta t$ corresponding to

$${}^{t+\Delta t}\mathbf{U} = {}^{t+\gamma\Delta t}\mathbf{U} + (1-\gamma)(\Delta t)\,{}^{t+\gamma\Delta t}\dot{\mathbf{U}} + (0.5)(1-\gamma)^2(\Delta t)^2\,{}^{t+\gamma\Delta t}\ddot{\mathbf{U}} \tag{10}$$

Next we use Eqs. (5) and (6), to obtain the velocity and displacement vectors at $t + \Delta t$.

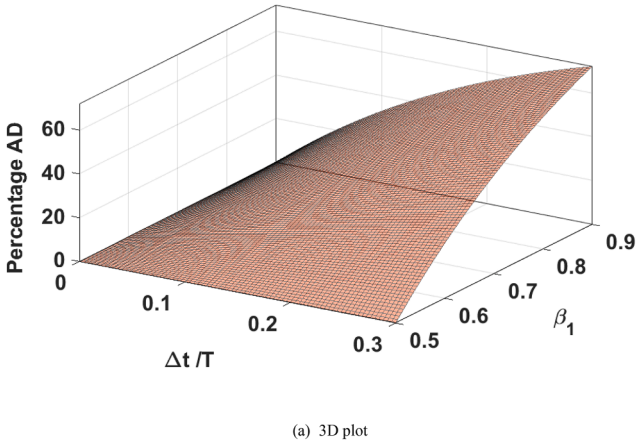

(a) 3D plot

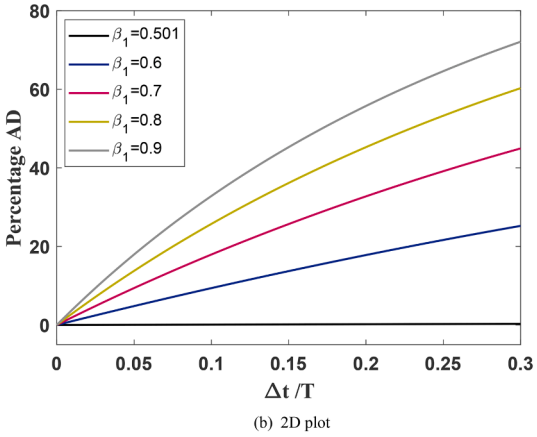

(b) 2D plot

Fig. 7. Amplitude decay of the explicit β_1/β_2-Bathe method for $\beta_2 = 0$ (first-order accuracy).

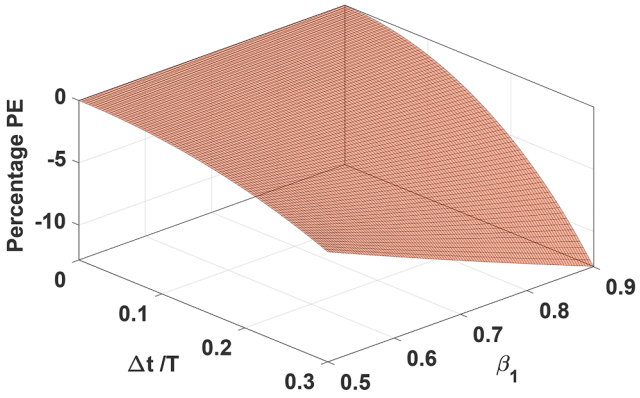

(a) 3D plot

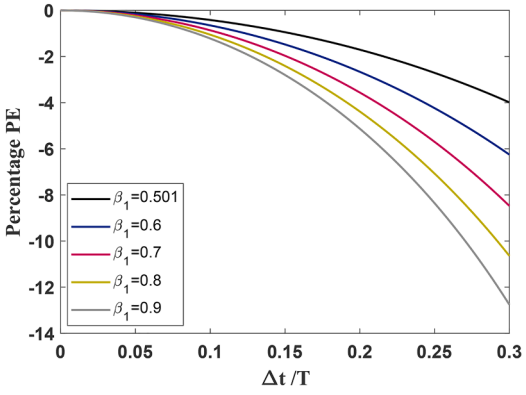

(b) 2D plot

Fig. 8. Period elongation of the explicit β_1/β_2-Bathe method for $\beta_2 = 0$ (first-order accuracy).

3. To determine the control parameters (γ, β_1 and β_2)

In Ref. [1], we introduced how the β_1/β_2-Bathe method can be used as a first-order or second-order solution procedure. We used $\gamma = 0.5$ and reasonable values of β_1 and β_2. Good solution results were obtained. However, we did not deeply pursue to find the optimal values for these two parameters β_1 and β_2 to reach the best solution accuracy.

When trying to establish the optimal values of β_1, β_2 and γ, we found that using $\gamma = 0.5$ is appropriate. However, the values of the parameters β_1 and β_2 should be different from those used earlier [1] in order to reach even better accuracy in some problem solutions.

If we consider the characteristic polynomial of the integration approximation (or amplification) matrix $\mathbf{A}$ for a direct time integration method, we obtain from $\det(\mathbf{A} - \lambda\mathbf{I}) = 0$

$$\lambda^3 - A_1\lambda^2 + A_2\lambda - A_3 = 0 \tag{11}$$

The stability criteria of Routh-Hurwitz are defined as

$$\begin{aligned} a_0 &= (1 + A_1 + A_2 + A_3) \geqslant 0 \\ a_1 &= (3 + A_1 - A_2 - 3A_3) \geqslant 0 \\ a_2 &= (3 - A_1 - A_2 + 3A_3) \geqslant 0 \\ a_3 &= (1 - A_1 + A_2 - A_3) \geqslant 0 \\ & (a_1 a_2 - a_3 a_0) \geqslant 0 \end{aligned} \tag{12}$$

where λ is an eigenvalue of the amplification matrix, and $A_1 = \text{trace}(\mathbf{A})$, $A_2 = 0.5\left[(\text{trace}(\mathbf{A}))^2 - \text{trace}(\mathbf{A}^2)\right]$ and $A_3 = \det(\mathbf{A})$ are the invariants of the matrix.

In (12), the first four conditions are the necessary conditions and the last condition is a sufficient condition for stability. The inequalities (12) can be used to establish the stability region of a solution scheme.

In the following, we use these criteria to study the second-order and first-order schemes. The amplification matrix of the explicit β_1/β_2-Bathe method is given in Ref. [1]. We first assume that physical damping is not included and thereafter (in Section 4) consider the effect of physical damping.

3.1. Recommendations for the second-order accurate scheme

As we discussed in Ref. [1], in the explicit β_1/β_2-Bathe method we must use $\beta_1 = 0.5$ to achieve second-order accuracy. Regarding the stability when using $\beta_1 = 0.5$ and $\xi = 0$ the following expressions are obtained from (12)

$$\begin{aligned} a_0 &= \left(\frac{\beta_2^2}{4} + \frac{1}{16}\right)(\omega\Delta t)^4 - (\omega\Delta t)^2 + 4 \geqslant 0 \\ a_1 &= \left(-\frac{\beta_2^2}{4} + \frac{\beta_2}{4} + \frac{1}{16}\right)(\omega\Delta t)^4 - (\omega\Delta t)^2 + 4 \geqslant 0 \\ a_2 &= \left(-\frac{1}{16}\right)(\omega\Delta t)^4 + (\omega\Delta t)^2 \geqslant 0 \\ a_3 &= \left(-\frac{\beta_2^2}{4} - \frac{1}{16}\right)(\omega\Delta t)^4 + (\omega\Delta t)^2 \geqslant 0 \\ (a_1 a_2 - a_3 a_0) &= \frac{1}{32}\left(\beta_2\left(2\beta_2^2 + \beta_2\right)\right)(\omega\Delta t)^8 - \left(\frac{\beta_2^2}{2}\right)(\omega\Delta t)^6 + \beta_2(\omega\Delta t)^4 \geqslant 0 \end{aligned} \tag{13}$$

where the frequency ω, the time step Δt and control parameter β_2 are all positive.

Considering the above inequalities leads to the following

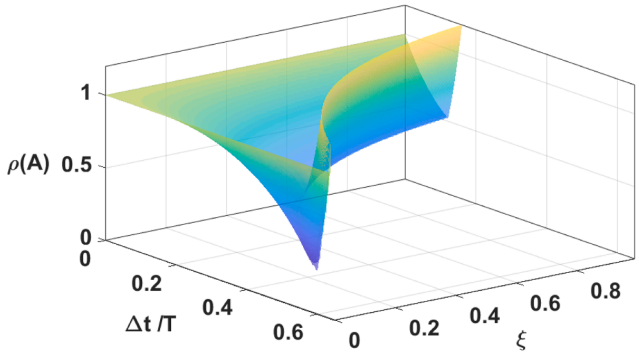

(a) 3D plot

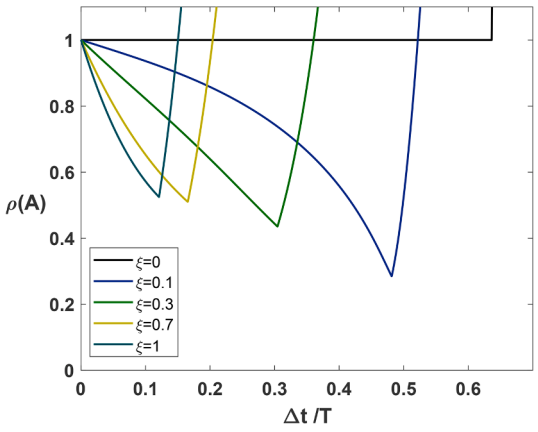

(b) 2D plot

Fig. 9. Spectral radius of the explicit β_1/β_2-Bathe method in the presence of physical damping $0 \leqslant \xi < 1$ for $\beta_1 = 0.5$ and $\beta_2 = 0$.

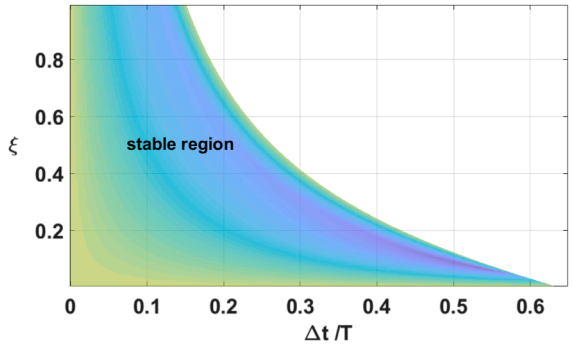

Fig. 10. Stable region of the explicit β_1/β_2-Bathe method in the presence of physical damping $0 \leqslant \xi < 1$ for $\beta_1 = 0.5$ and $\beta_2 = 0$.

observations.

The expression $a_0 \geqslant 0$ is satisfied for $\beta_2 \geqslant 0$ for every $(\omega\Delta t) \geqslant 0$. The condition $a_1 \geqslant 0$ is satisfied for $\beta_2 \geqslant 0$ when $0 \leqslant (\omega\Delta t) \leqslant \sqrt{\frac{8}{1+\sqrt{4\beta_2^2-4\beta_2}}}$. The condition $a_2 \geqslant 0$ is satisfied for $\beta_2 \geqslant 0$ when $0 \leqslant (\omega\Delta t) \leqslant 4$. The condition $a_3 \geqslant 0$ is satisfied for $\beta_2 \geqslant 0$ when $0 \leqslant (\omega\Delta t) \leqslant \frac{4}{\sqrt{4\beta_2+1}}$. The condition $(a_1 a_2 - a_3 a_0) \geqslant 0$ is satisfied if $\beta_2 \geqslant 0$ for every $(\omega\Delta t) \geqslant 0$. The five criteria in the conditions (13) are simultaneously satisfied for $\beta_2 \geqslant 0$ with $0 \leqslant (\omega\Delta t) \leqslant \frac{4}{\sqrt{4\beta_2+1}}$.

In summary, the Routh-Hurwitz criteria show that the explicit β_1/β_2-Bathe method for $\beta_1 = 0.5$ is conditionally stable provided

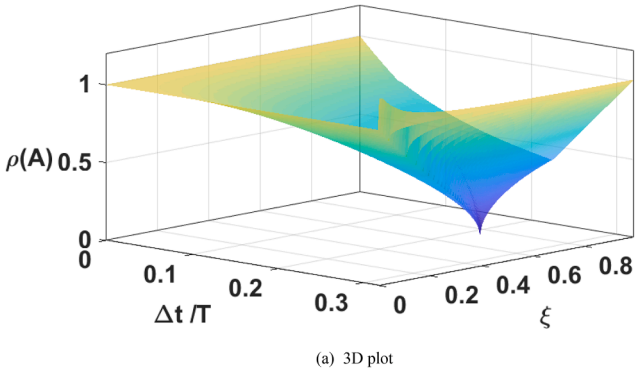

(a) 3D plot

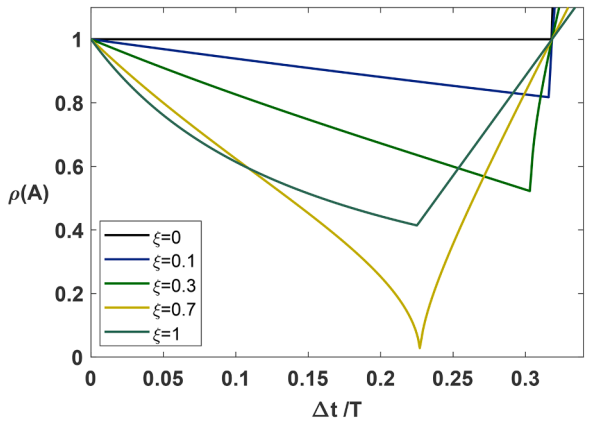

(b) 2D plot

Fig. 11. Spectral radius of the CDM in the presence of physical damping $0 \leqslant \xi < 1$.

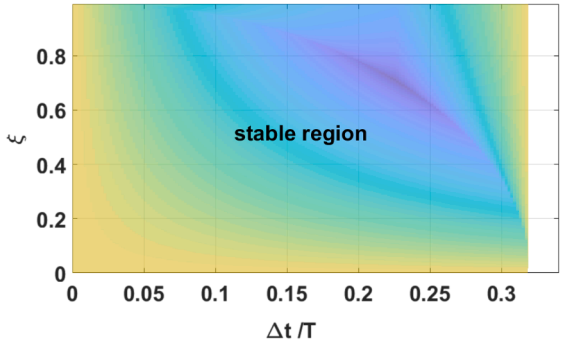

Fig. 12. Stable region of the CDM in the presence of physical damping $0 \leqslant \xi < 1$ The spectral radius is smaller at darker color.

Table 1a
Values of parameters β_1 and β_2 generally giving reasonably accurate results.

For wave propagations	For structural dynamics
$\beta_1 = 0.54$, $\beta_2 = 0$	$\beta_1 = 0.5$, $\beta_2 = 0.04$

Table 1b
Ranges of values of parameters β_1 and β_2 to choose for very good results.

For wave propagations	For structural dynamics
$0.5 < \beta_1 \leqslant 0.9$, $\beta_2 = 0$	$\beta_1 = 0.5$, $0 \leqslant \beta_2 \leqslant 0.2$

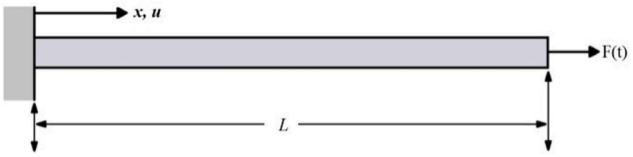

Fig. 13. A clamped–free bar subjected to a step end load [17].

$$\beta_2 \geqslant 0\ , \quad 0 \leqslant (\omega \Delta t) \leqslant \frac{4}{\sqrt{4\beta_2 + 1}} \tag{14}$$

Hence in this case the critical time step Δt_{cr} for second-order accuracy is

$$\Delta t_{cr} = \left(\frac{1}{\omega_h}\right) \frac{4}{\sqrt{4\beta_2 + 1}} \tag{15}$$

where ω_h is the highest frequency and $T_s = \frac{2\pi}{\omega_h}$ is the smallest period of the finite-element mesh.

Based on the above results and the results shown in Figs. 1–4, we recommend to use

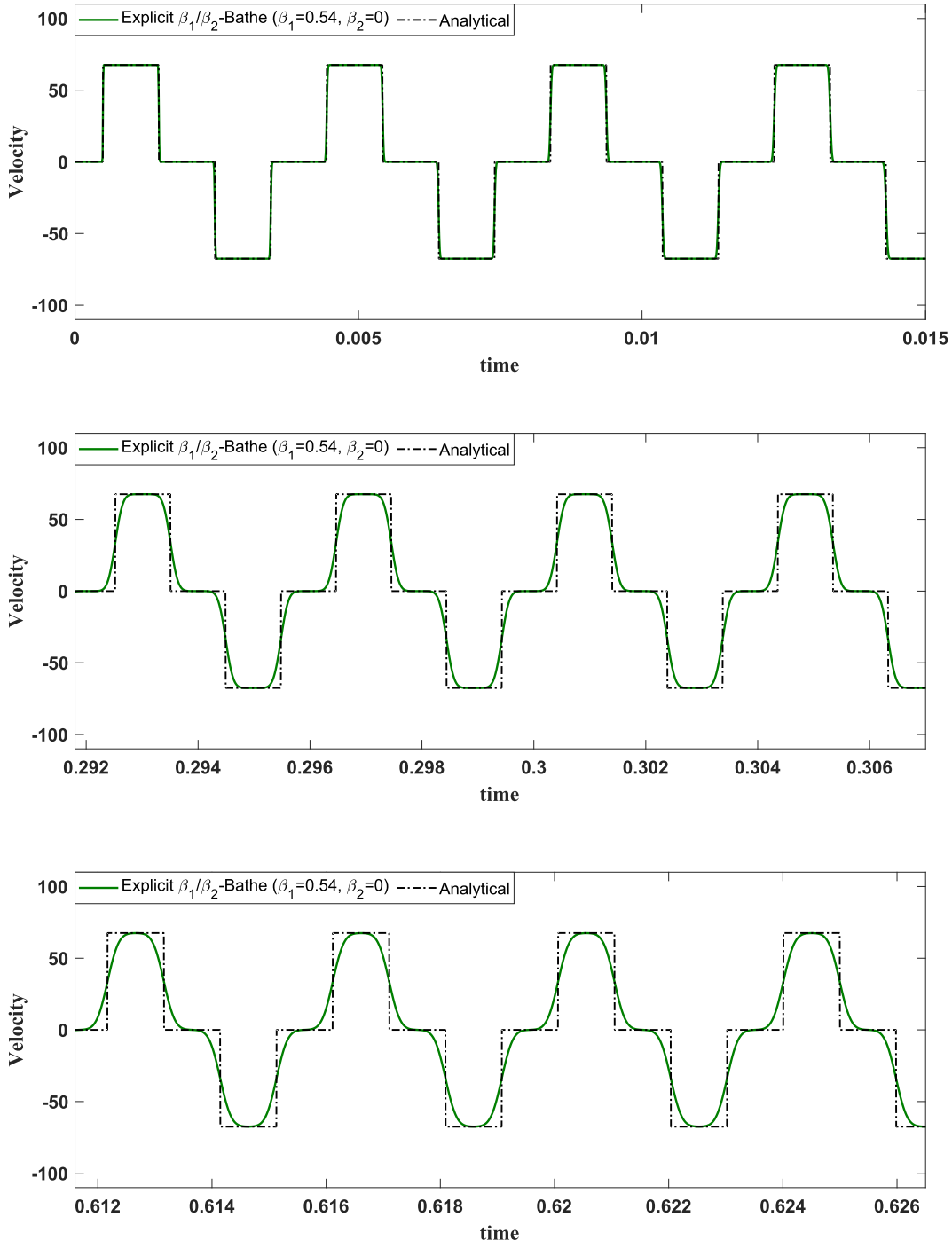

Fig. 14. Predicted velocity at the mid-point of the bar,CFL = 1.925

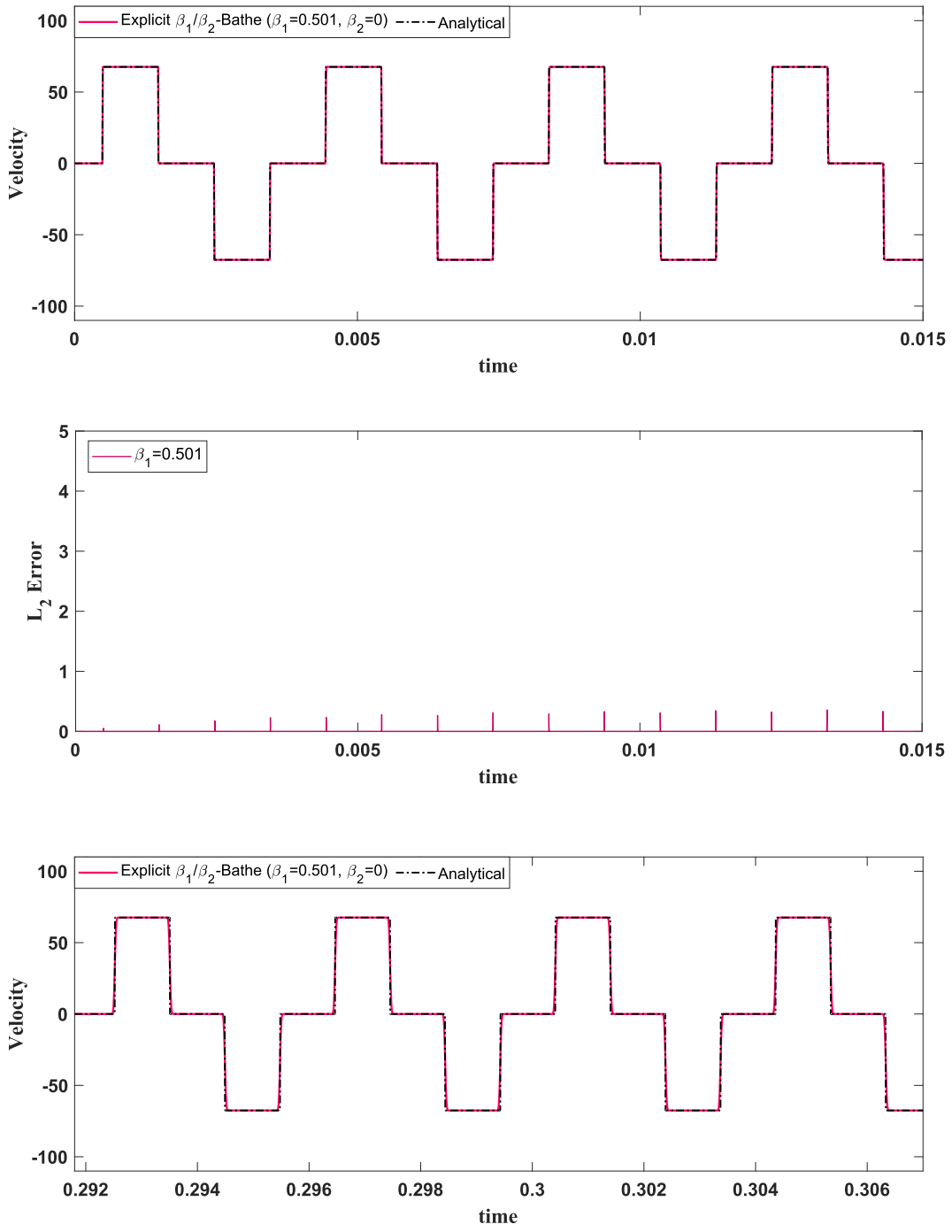

Fig. 15. Predicted velocity and relative L_2 error at the mid-point of the bar,CFL $= 1.998$

$$\beta_1 = 0.5\,, \quad 0 \leqslant \beta_2 \leqslant 0.2 \tag{16}$$

The spectral radius, amplitude decay and period elongation are shown in Figs. 1–4. As we see in Fig. 1, the spectral radius indicates that by choosing a larger β_2, numerical damping is already applied for a smaller time step, but Figs. 1 and 2 show that with an increasing value of β_2, the stability region decreases. Fig. 3 gives the amplitude decay which is zero when $\beta_2 = 0$ and is maximum when $\beta_2 = 0.2$, and Fig. 4 shows the period elongation which for $\beta_2 = 0$ is negative and for $\beta_2 = 0.2$ positive.

3.2. Recommendations for the first-order accurate scheme

We concluded in Ref. [1] that for the solution of wave propagation problems, in addition to using the first-order accurate scheme of the method, we need that the spectral radius decreases (from the value of 1)

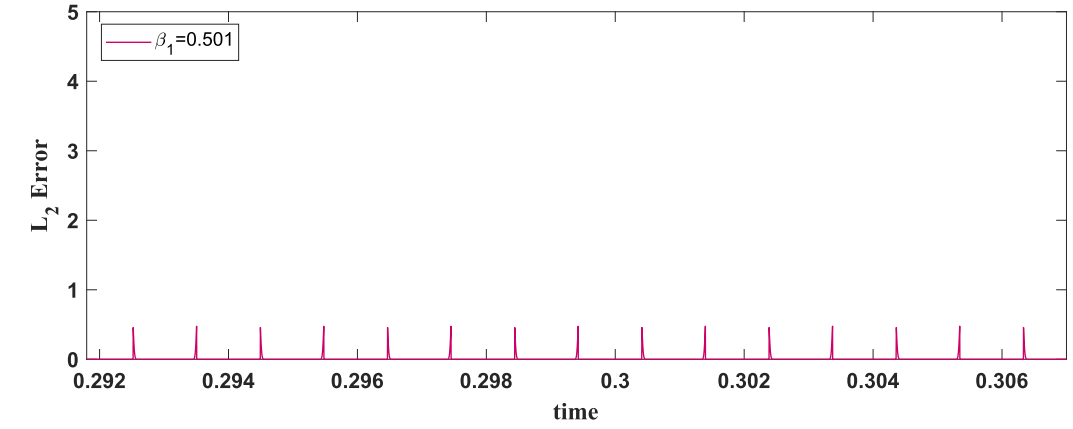

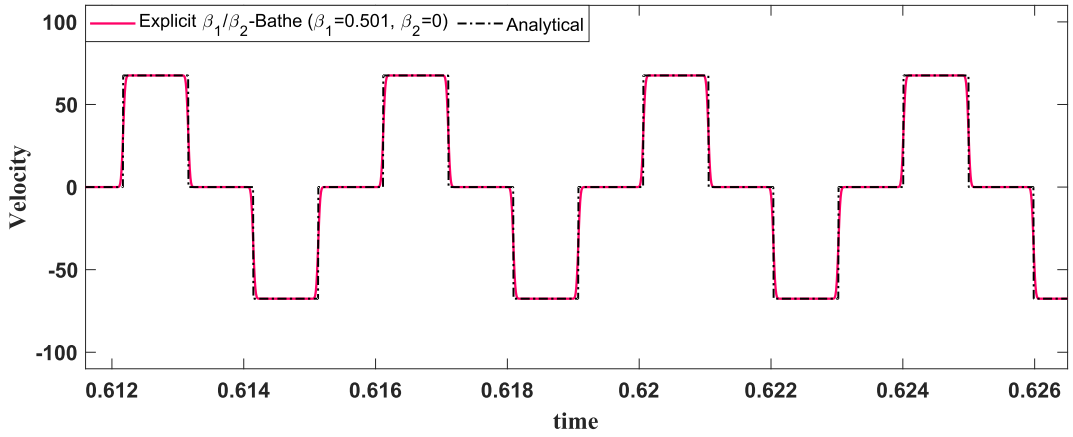

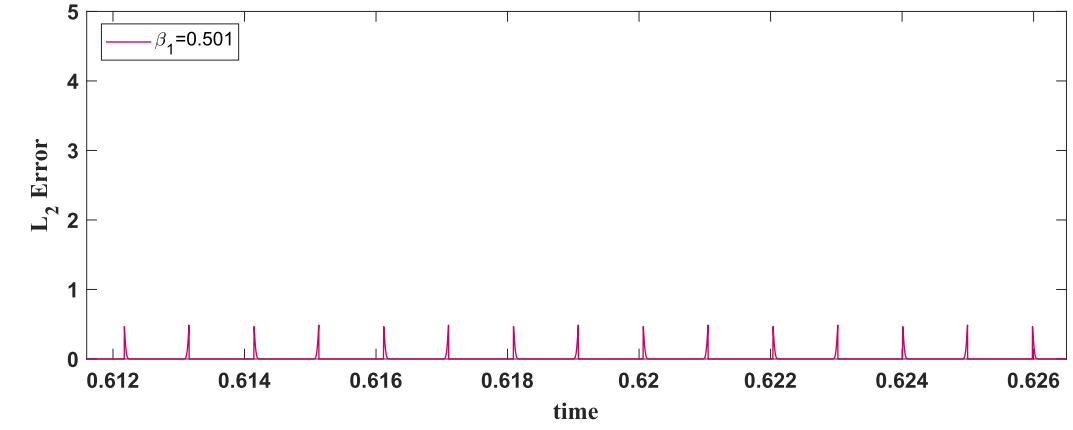

Fig. 15. (*continued*).

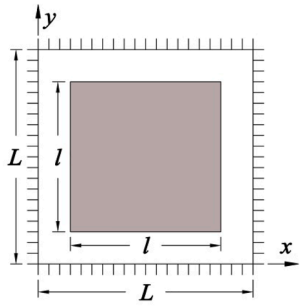

Fig. 16. The square membrane with wave velocity $c = 10\ m/s$[1].

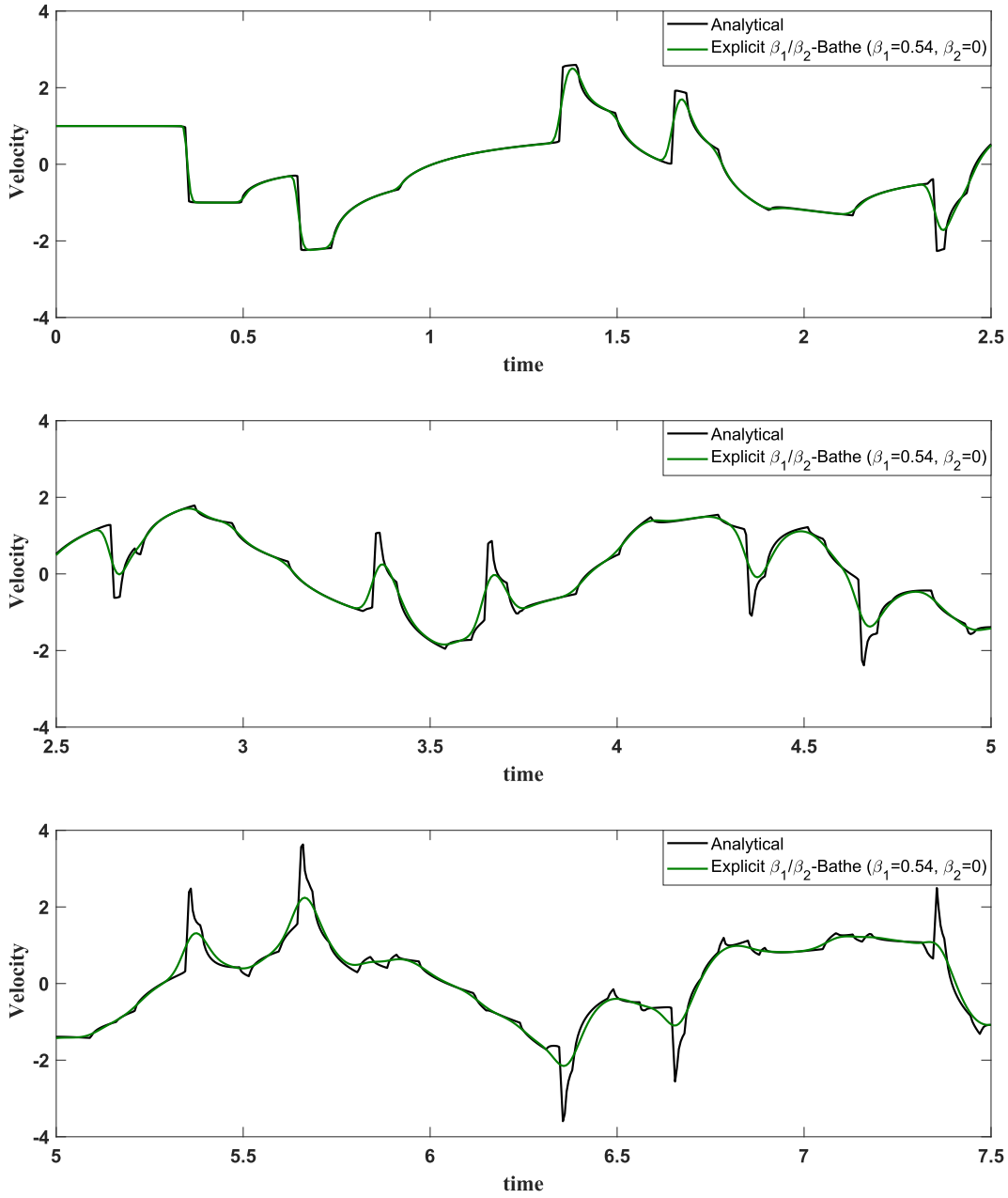

Fig. 17. Predicted velocity at center point,CFL $= 1.925$

already at a small time step but then continues to decrease with a very small slope. If the decrease of the spectral radius is small even at relatively large time steps, it allows to use large time steps for an accurate solution. Of course, the period elongation error should also be reasonably small.

In the explicit β_1/β_2-Bathe method we need to use $\beta_1 \neq 0.5$ to achieve first-order accuracy, and we select $\beta_2 = 0$ to have the spectral radius decrease as explained above.

Considering the stability when $\beta_2 = 0$ and $\xi = 0$, we obtain the conditions

$$
\begin{aligned}
a_0 &= (\frac{\beta_1^2}{8} + \frac{1}{32})(\omega\Delta t)^4 - (\beta_1 + \frac{1}{2})(\omega\Delta t)^2 + 4 \geqslant 0 \\
a_1 &= (\frac{\beta_1}{8})(\omega\Delta t)^4 - (\omega\Delta t)^2 + 4 \geqslant 0 \\
a_2 &= (-\frac{\beta_1^2}{8} - \frac{1}{32})(\omega\Delta t)^4 + (\beta_1 + \frac{1}{2})(\omega\Delta t)^2 \geqslant 0 \\
a_3 &= (-\frac{\beta_1}{8})(\omega\Delta t)^4 + (\omega\Delta t)^2 \geqslant 0 \\
(a_1 a_2 - a_3 a_0) &= -\frac{1}{8}(2\beta_1 - 1)^2(\omega\Delta t)^4 + (4\beta_1 - 2)(\omega\Delta t)^2 \geqslant 0
\end{aligned}
\tag{17}
$$

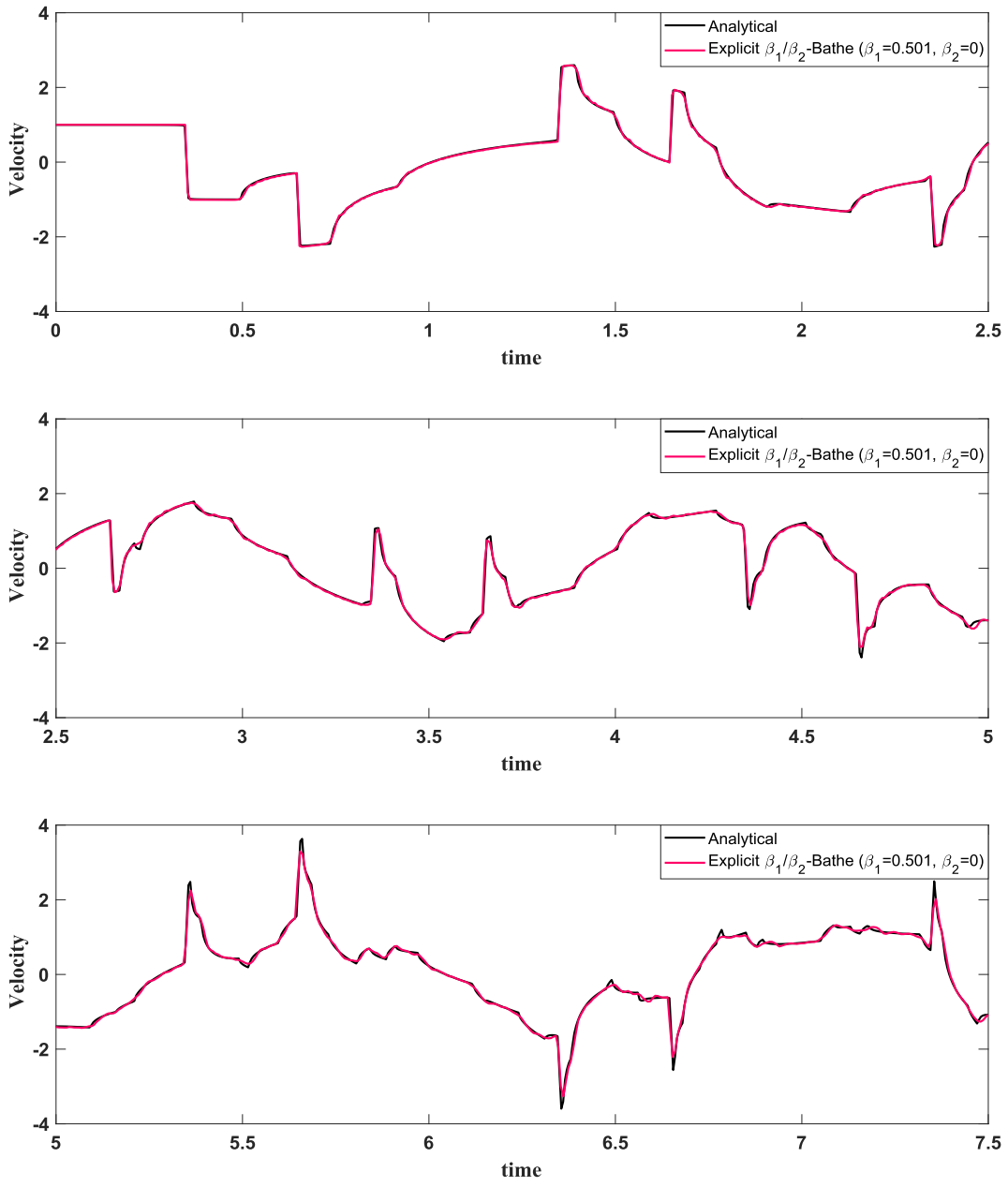

Fig. 18. Predicted velocity at center point,CFL = 1.998

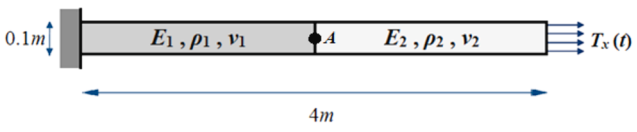

Fig. 19. A bi-material rod subjected to a step traction at its right edge [1].

Considering the above inequalities leads to the following observations. The expression $a_0 \geqslant 0$ is satisfied when $\beta_1 \geqslant 0$ for every $(\omega\Delta t) \geqslant 0$. The condition $a_1 \geqslant 0$ is satisfied when $\beta_1 \geqslant \frac{1}{2}$ for every $(\omega\Delta t) \geqslant 0$, and also for $\beta_1 < \frac{1}{2}$ provided $0 \leqslant (\omega\Delta t) \leqslant 2\sqrt{\frac{1-\sqrt{1-2\beta_1}}{\beta_1}}$ and $(\omega\Delta t) \geqslant 2\sqrt{\frac{1+\sqrt{1-2\beta_1}}{\beta_1}}$. The condition $a_2 \geqslant 0$ is satisfied when $\beta_1 \geqslant 0$ for $0 \leqslant (\omega\Delta t) \leqslant 4\sqrt{\frac{2\beta_1+1}{4\beta_1^2+1}}$. The condition $a_3 \geqslant 0$ is satisfied when $\beta_1 \geqslant 0$ for $0 \leqslant (\omega\Delta t) \leqslant \sqrt{\frac{8}{\beta_1}}$. The condition $(a_1 a_2 - a_3 a_0) \geqslant 0$ is satisfied when $\beta_1 \geqslant \frac{1}{2}$ for $0 \leqslant (\omega\Delta t) \leqslant 4\sqrt{\frac{1}{(2\beta_1-1)}}$. The five criteria in equation (17) are simultaneously satisfied when $\beta_2 \geqslant 0$ for $0 \leqslant (\omega\Delta t) \leqslant \frac{4}{\sqrt{4\beta_2+1}}$.

In summary, the Routh- Hurwitz criteria show that the explicit β_1/β_2-Bathe method for $\beta_2 = 0$ and $\beta_1 \neq 0.5$ is conditionally stable provided

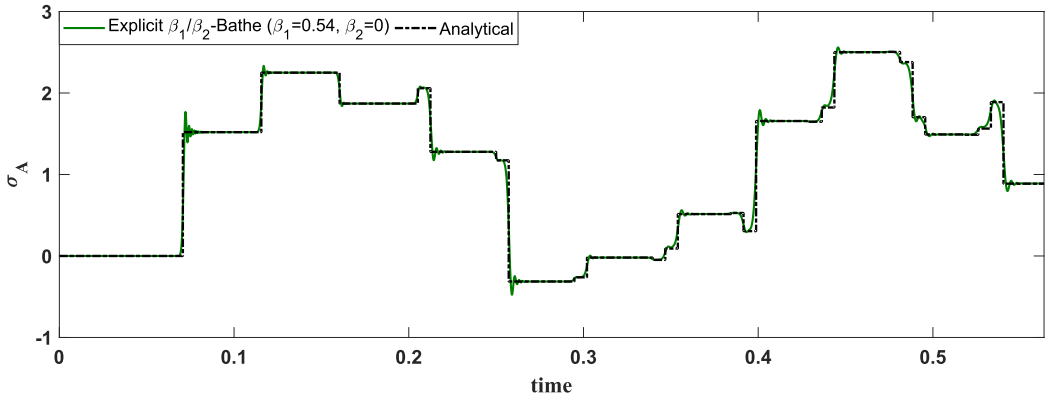

a. Predicted stress at point A, CFL = 1. 925

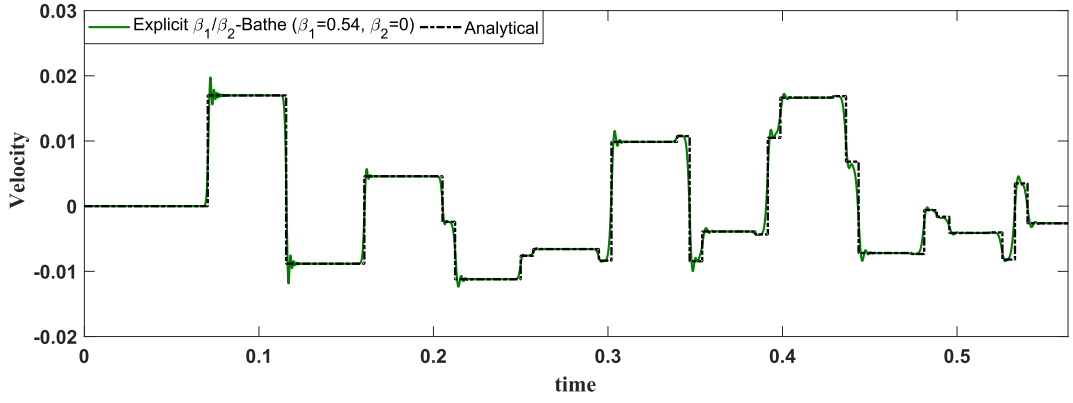

b. Predicted velocity at point A, CFL = 1.925

Fig. 20. (a) Predicted stress at point A, CFL = 1. 925. (b) Predicted velocity at point A, CFL = 1.925.

$$\beta_1 > \frac{1}{2} \text{ and } 0 \leqslant (\omega \Delta t) \leqslant \sqrt{\frac{8}{\beta_1}} \tag{18}$$

The critical time step Δt_{cr} of the explicit β_1/β_2-Bathe method when used with first-order accuracy is

$$\Delta t_{cr} = \left(\frac{1}{\omega_h}\right)\sqrt{\frac{8}{\beta_1}} \tag{19}$$

Based on the above results and the results shown in Figs. 5–8, we recommend to use

$$\beta_2 = 0\,, \quad 0.5 < \beta_1 \leqslant 0.9 \tag{20}$$

Figs. 5–8 show the spectral radius, stability region, amplitude decay and period elongation of the scheme. Fig. 5 of the spectral radius shows that by choosing a larger β_1, numerical damping can be applied earlier. Fig. 6 displays that the stable region diminishes as the value of β_1 increases. As seen in Figs. 7 and 8, as we increase the value of β_1, both, the amplitude decay error and the period elongation error increase.

4. Stability of the explicit β_1/β_2-Bathe method in the presence of physical damping, with $0 \leqslant \xi < 1$

Having identified values to use for the two parameters β_1 and β_2, we next investigate the stability of the explicit β_1/β_2-Bathe method for these values in the presence of physical damping. Using the conditions in (12) and the results of Section 3, we find that the method is stable for $\xi \neq 0$ in the two introduced regions for $\Delta t \leqslant \Delta t_{cr}$ with

$$\Delta t_{cr} = \left(\frac{1}{\omega_h}\right)\frac{\left(-0.5\xi - \xi\beta_1 + \sqrt{\left(0.5\beta_1 + \beta_2 + (0.5\xi + \xi\beta_1)^2\right)}\right)}{(0.25\beta_1 + 0.5\beta_2)} \tag{21}$$

Hence the critical time step to use depends on the value of ξ.

It is of value to compare this result with the result for the central difference method (CDM) when physical damping is included, for $0 \leqslant \xi < 1$.

For this comparison, we consider the case $\beta_1 = 0.5$ and $\beta_2 = 0$ in the explicit β_1/β_2-Bathe method. We select these parameters to have no numerical damping, like when using the CDM.

Figs. 9 and 10 show that for the explicit β_1/β_2-Bathe method, the stability range of the method decreases as the physical damping increases, whereas for the CDM, Figs. 11 and 12 show that the spectral radius decreases at small time step with increasing physical damping, but the stability range of the method remains the same. The inherent reason is that the β_1/β_2-Bathe method is fully explicit because the physical damping is represented on the right-hand side of the governing equations, Eqs. (1) and (4). On the other hand, in the CDM, the physical damping effect, the damping matrix **C**, appears on the left-hand side of the governing equation [2]. This is like in an implicit time integration scheme and renders the stability region of the CDM independent of ξ

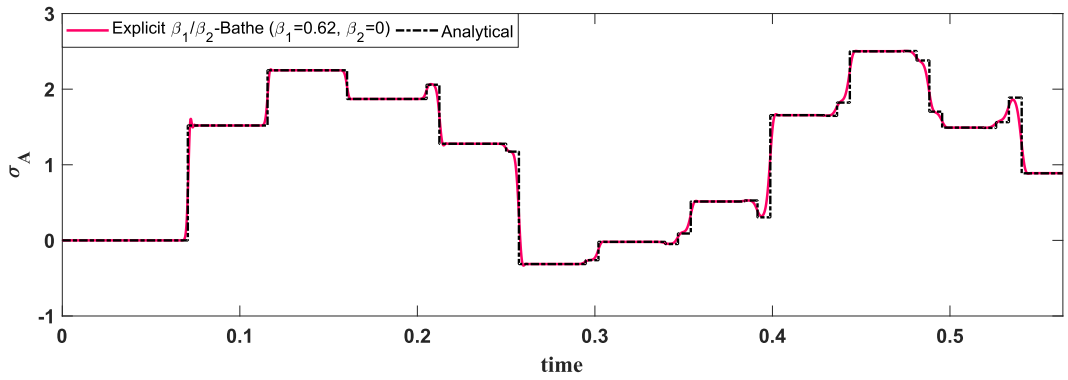

a. Predicted stress at point A, CFL = 1. 8

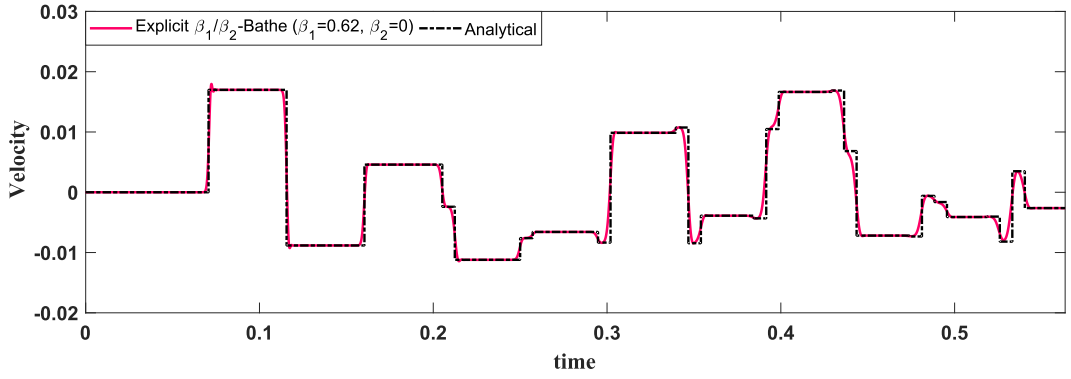

b. Predicted velocity at point A, CFL = 1.8

Fig. 21. (a) Predicted stress at point A, CFL = 1.8. (b) Predicted velocity at point A, CFL = 1.8.

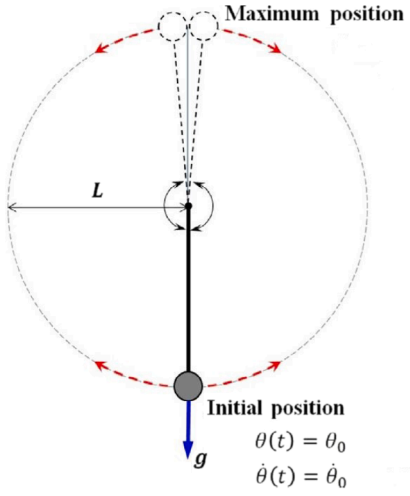

Fig. 22. Configuration of oscillating simple pendulum [30].

(although implicit schemes can also be unstable for certain values of their parameters [2]). But of course, as ξ increases, using a fixed time step satisfying stability, the accuracy of solution decreases in both solution schemes.

5. Illustrative example solutions

We first reconsider in Section 5.1 the solutions of three linear example problems, solved earlier with the explicit β_1/β_2-Bathe method [1]. The results, when compared with those given in ref. [1], show the improvements in solutions reached using the parameter values recommended above.

Then we illustrate in Section 5.2 the use of the explicit β_1/β_2-Bathe method in solving some nonlinear problems that have also been considered before [30–33].

For the solutions using the explicit β_1/β_2-Bathe method, we recommend to use the values given in Table 1a. However, to obtain an optimal solution, the user should choose values from the ranges given in Table 1b. With values within these regions, very good response predictions may be obtained (even for a response of long time).

5.1. Linear systems

The linear solutions given below illustrate the remarkable accuracy that can be obtained.

5.1.1. A clamped bar subjected to a step-end load

We consider the clamped bar shown in Fig. 13 with the material and geometric properties $E = 30 \times 10^6$ *psi*, $\rho = 0.00073$ lb/in^3,$A = 1$ in^2, and $L = 200$ *in*. The applied step end load is F(t) = 10,000 *lb*. We use 1000 equal 2-node elements and the lumped mass matrix to model the

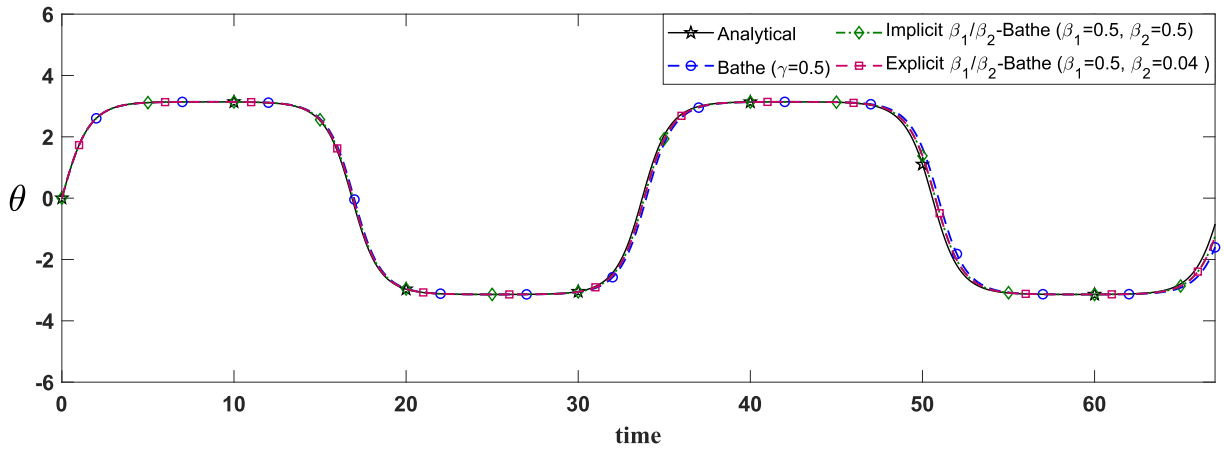

Fig. 23. Predicted angular displacement $\Delta t = 0.001$.

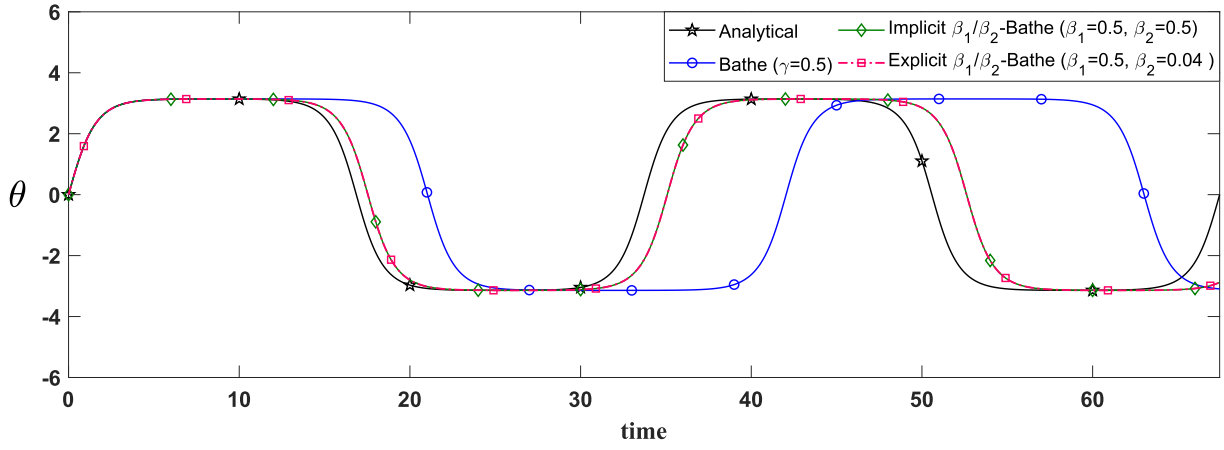

Fig. 24. Predicted angular displacement $\Delta t = 0.003$.

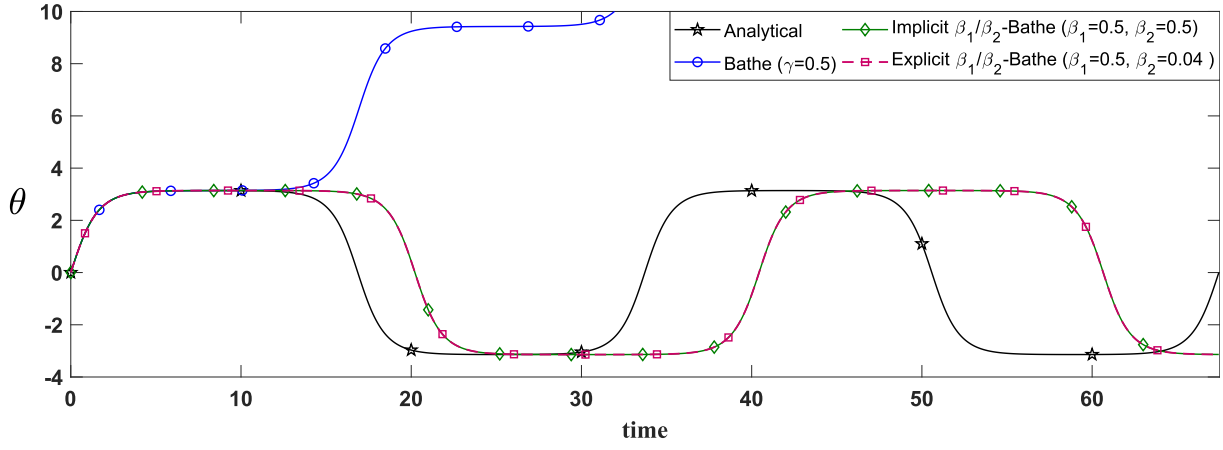

Fig. 25. Predicted angular displacement $\Delta t = 0.0042$.

bar and have $T_s = 3.099422668 \times 10^{-6}$.

Using $\beta_1 = 0.54$ and $\beta_2 = 0$ from Table 1a, and $c = \sqrt{\frac{E}{\rho}}$, the CFL number and time step are given by

$$\text{CFL} = (\frac{c}{\Delta x})(\frac{T_s}{2\pi})\frac{\sqrt{8}}{\sqrt{\beta_1}} = 1.925$$

$$\Delta t = \text{CFL}(\frac{\Delta x}{c}) = 1.925 \times (\frac{\frac{200}{1000}}{\sqrt{\frac{30\times 10^6}{0.00073}}})$$

To improve the solution results we choose the values of parameters from Table 1b and select $\beta_1 = 0.501$. Thus we have

$$\text{CFL} = (\frac{c}{\Delta x})(\frac{T_s}{2\pi})\frac{\sqrt{8}}{\sqrt{\beta_1}} = 1.998$$

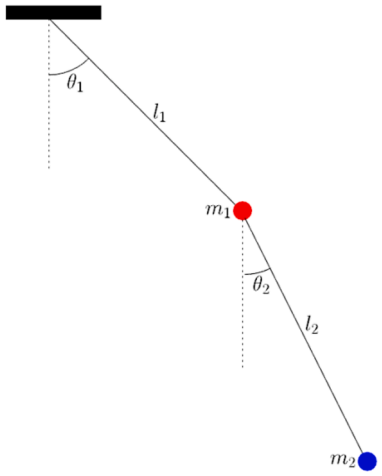

Fig. 26. The double pendulum, $m_1 = m_2 = 2$ *kg*, $l_1 = l_2 = 2$ *m* and $g = 9.81$ m/s^2.

$$\Delta t = \text{CFL}(\frac{\Delta x}{c}) = 1.998 \times (\frac{\frac{200}{1000}}{\sqrt{\frac{30\times10^6}{0.00073}}})$$

Figs. 14 and 15 give the predicted velocity responses at the mid-point of the bar (node 500) using the explicitβ_1/β_2-Bathe method. In these figures, we depict the response in the time intervals [0, 0.015], [0.2918, 0.307] and [0.6116, 0.6266] giving the calculated velocity in comparison to the analytical solution. Using $\beta_1 = 0.54, \beta_2 = 0$ the accuracy of the solution is excellent in the short time response but then deteriorates. Then using $\beta_1 = 0.501, \beta_2 = 0$ the solution is remarkably accurate over the complete time interval although the time step used is even slightly larger. These curves show the remarkable accuracy reached. However, since the analytical solution for certain time ranges is zero, the relative actual error measured on the analytical solution is mathematically difficult to express. Nevertheless, in Fig. 15 we show the relative L_2 error assuming that it is zero when the analytical solution is zero. We see that there are only small peaks in the error at the sudden changes in velocity.

5.1.2. *Prestressed square membrane*

We consider the prestressed square membrane with $L = 10$ m shown in Fig. 16 subjected to a constant initial velocity prescribed over its

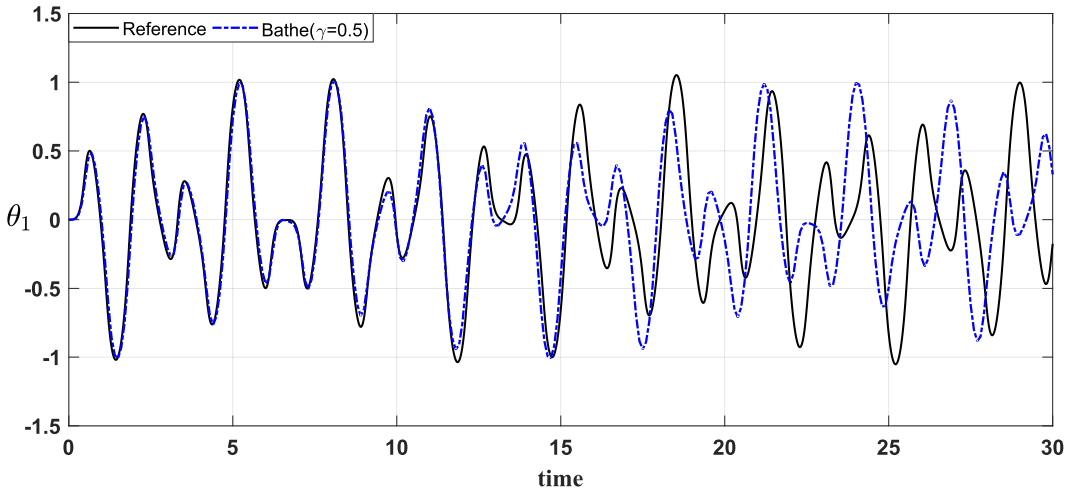

(a) θ_1

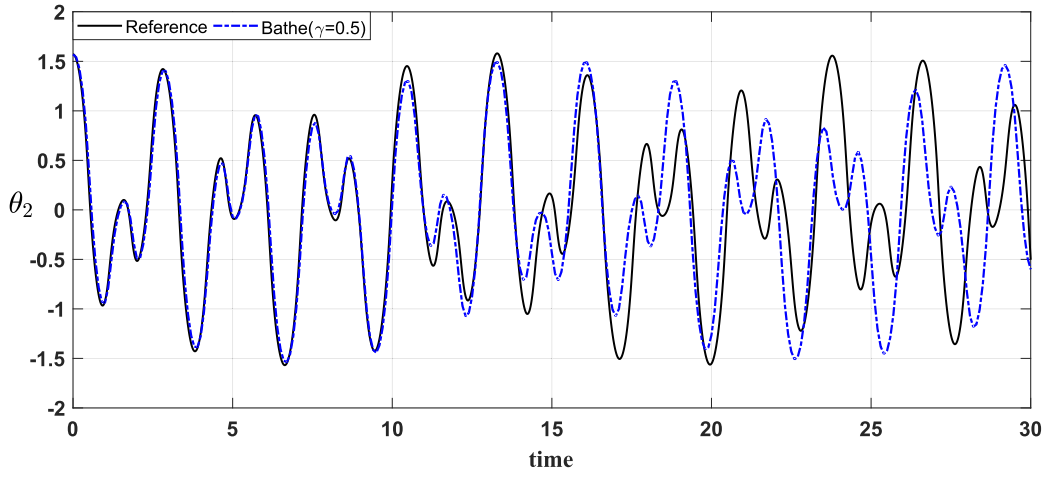

(b) θ_2

Fig. 27. Predicted angular displacements using standard Bathe method with $\Delta t = 0.1$.

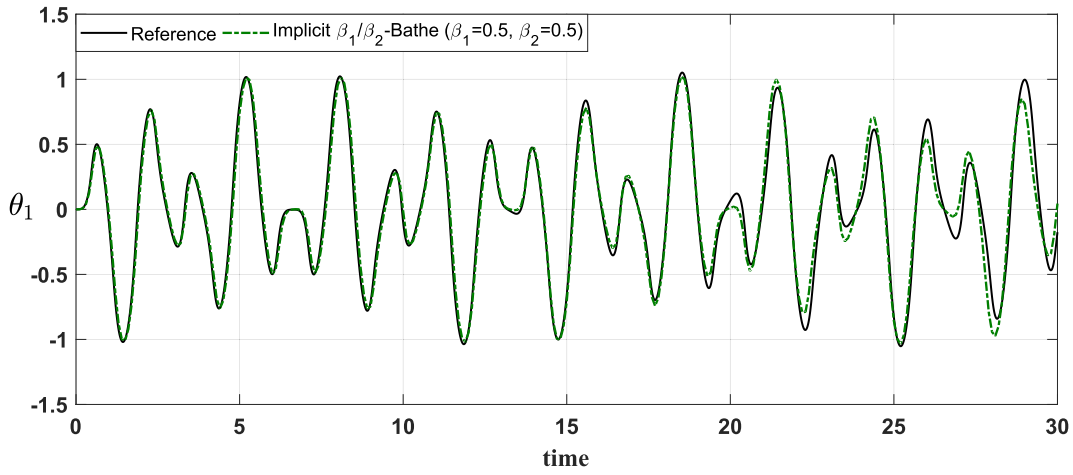

(a) θ_1

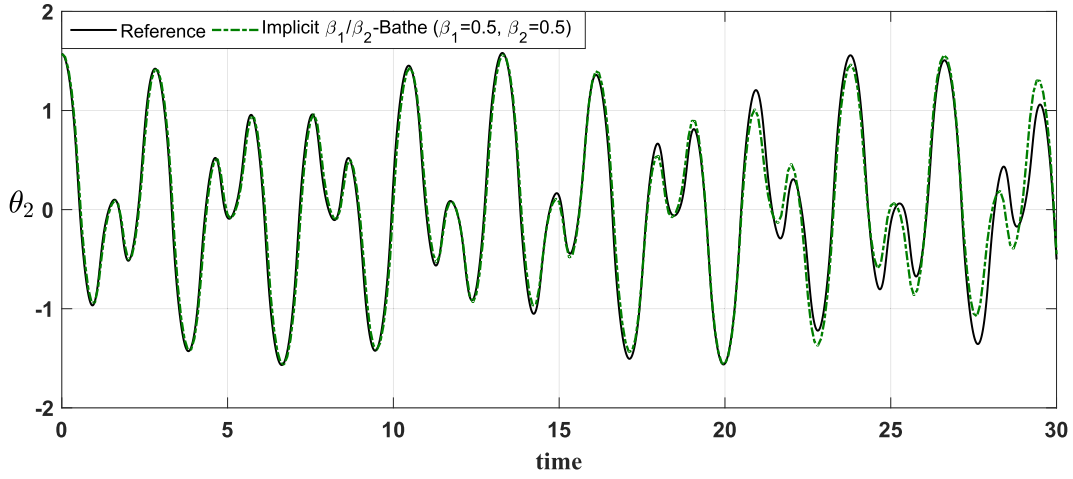

(b) θ_2

Fig. 28. Predicted angular displacements using implicit β_1/β_2-Bathe method with $\Delta t = 0.1$.

central domain of $l \times l$, $l = 7$ m [1]. Due to symmetry, we only discretize a quarter of the membrane using 150 × 150 4-node elements and have $T_s = 0.010472167$.

Using first $\beta_1 = 0.54$ and $\beta_2 = 0$ we have

$$\text{CFL} = (\frac{c}{\Delta x})(\frac{T_s}{\pi})\frac{\sqrt{8}}{\sqrt{\beta_1}} = 1.925$$

$$\Delta t = \text{CFL}(\frac{\Delta x}{c}) = 1.925 \times \frac{1}{300}$$

Then to improve the results using $\beta_1 = 0.501$ and $\beta_2 = 0$ we have

$$\text{CFL} = (\frac{c}{\Delta x})(\frac{T_s}{\pi})\frac{\sqrt{8}}{\sqrt{\beta_1}} = 1.998$$

$$\Delta t = \text{CFL}(\frac{\Delta x}{c}) = 1.998 \times \frac{1}{300}$$

Figs. 17 and 18 show the prediction of the velocity response. Using $\beta_1 = 0.54$, $\beta_2 = 0$, the solution accuracy is very good initially but with $\beta_1 = 0.501$, $\beta_2 = 0$ we achieve an excellent response prediction throughout the time considered, and (as in Section 5.1.1) with the slightly larger time step.

5.1.3. *A bi-material rod subjected to a step end load*

Fig. 19 shows the rod we consider; it consists of two pieces with different material properties. The wave velocities of the left and right pieces are equal to $c_1 = 40\sqrt{5}$ m/s and $c_2 = 20\sqrt{2}$ m/s, respectively. The rod is at rest when suddenly a uniform constant step traction of unit magnitude is applied at its right end.

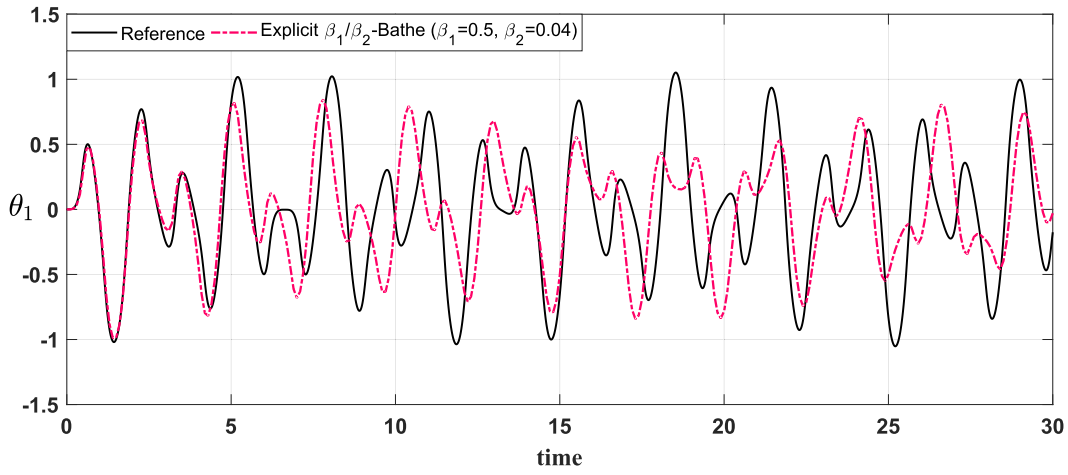

(a) θ_1

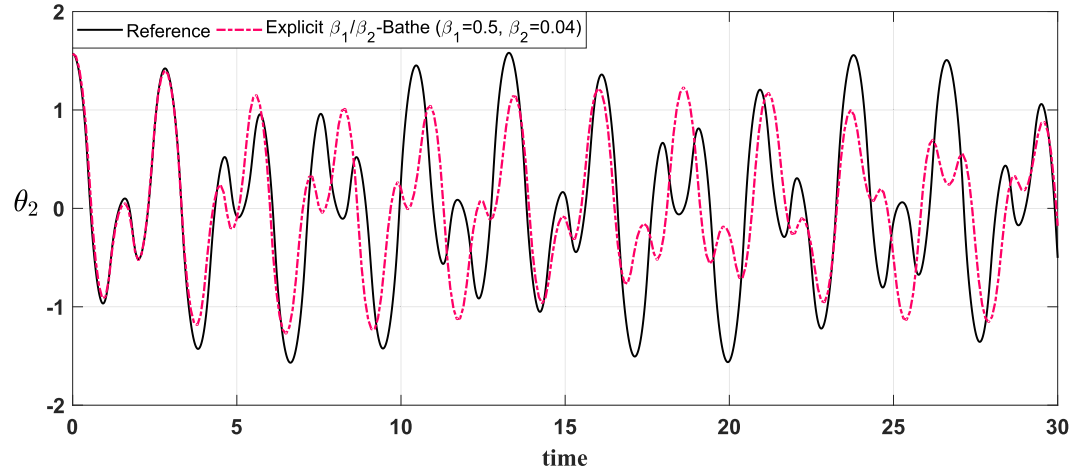

(b) θ_2

Fig. 29. Predicted angular displacements using explicit β_1/β_2-Bathe method with $\Delta t = 0.1$.

Using a mesh of 1×800 equal 4- node two-dimensional elements, with 400 elements in each piece of material and a lumped mass matrix we have $T_s = 5.56580819 \times 10^{-4}$.

Using $\beta_1 = 0.54$ and $\beta_2 = 0$, we have

$$\text{CFL} = (\frac{c_1}{\Delta x})(\frac{T_s}{2\pi})\frac{\sqrt{8}}{\sqrt{\beta_1}} = 1.925$$

$$\Delta t = \text{CFL}(\frac{\Delta x}{c_1}) = 1.925 \times \frac{0.005}{\sqrt{800}}$$

and selecting $\beta_1 = 0.62$ and $\beta_2 = 0$, we obtain

$$\text{CFL} = (\frac{c_1}{\Delta x})(\frac{T_s}{2\pi})\frac{\sqrt{8}}{\sqrt{\beta_1}} = 1.8$$

$$\Delta t = \text{CFL}(\frac{\Delta x}{c_1}) = 1.8 \times \frac{0.005}{\sqrt{800}}$$

The stress and velocity predictions at point A are shown in Figs. 20 and 21. We see that an accurate response prediction is obtained with a slightly better accuracy using $\beta_1 = 0.62$.

5.2. Nonlinear systems

In this section, we consider two nonlinear systems. For solving these nonlinear problems, we use the standard Bathe, implicit β_1/β_2-Bathe and the explicit β_1/β_2-Bathe methods.

In all problem solutions using the implicit methods, Newton–Raphson iterations are performed to solve the nonlinear equations in each time step, with the iterations performed until

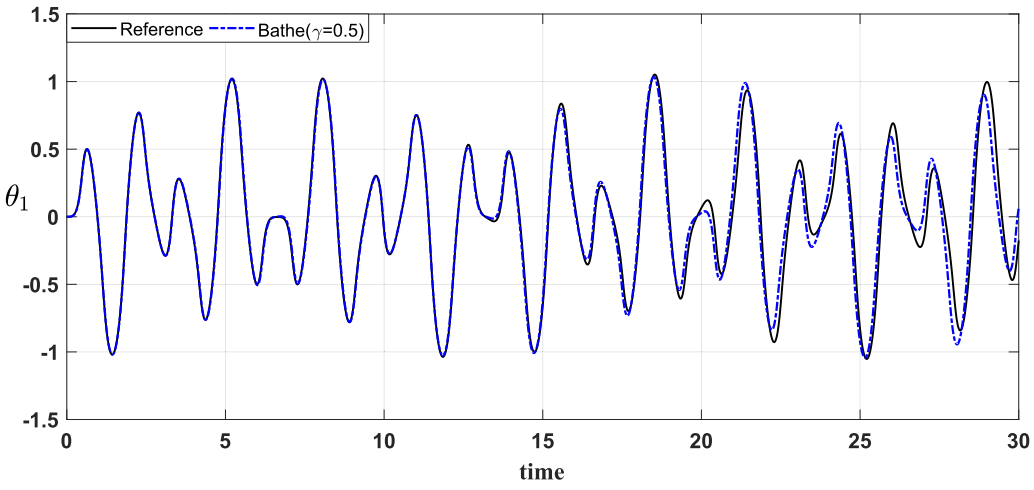

(a) θ_1

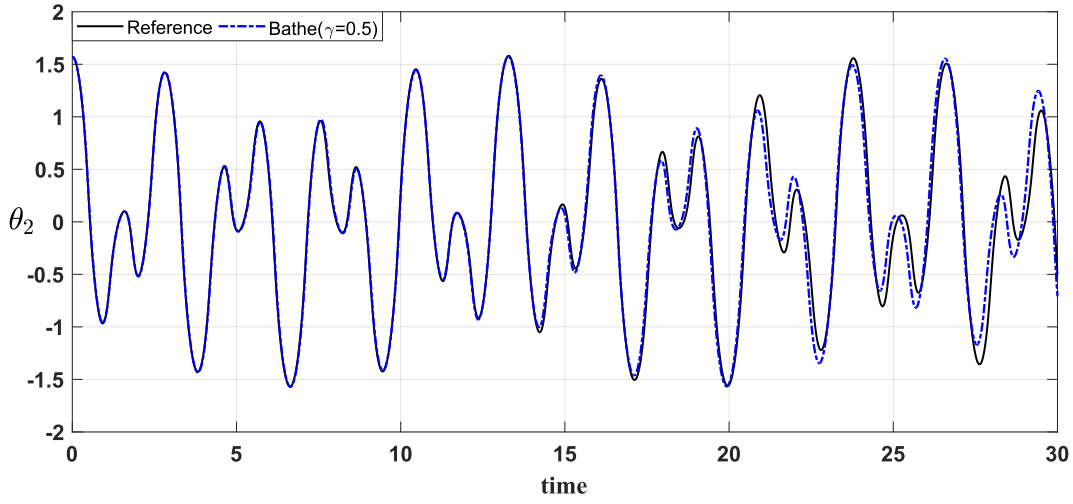

(b) θ_2

Fig. 30. Predicted angular displacements using standard Bathe method with $\Delta t = 0.01$.

$$\left\|\Delta \mathbf{U}^{(\mathbf{i})}\right\| < \varepsilon$$

where $\Delta \mathbf{U}^{(\mathbf{i})}$ is the displacement increment reached in iteration (i) and ε is the convergence tolerance, $\varepsilon = 10^{-5}$

5.2.1. *Oscillating simple pendulum*

We consider the "toy problem" of an oscillating simple pendulum. The system has been contrived for the initial conditions given and has been amply analyzed before [30–32].

The pendulum consists of a mass attached to a frictionless hinged weightless rod of length L, see Fig. 22. Dimensionless values $g = 1$ and $L = 1$ are used in the example, and the equation of motion is

$$\ddot{\theta} + (\frac{g}{L})\sin(\theta) = 0$$

where $\theta(t)$ is the angle between the rod at time t and a vertical line. The initial conditions are $\theta_0 = 0$ and $\dot{\theta}_0 = 1.999999238456499$.

To solve this problem we use $\Delta t = 0.001$, $\Delta t = 0.003$ and $\Delta t = 0.0042$. As expected, see Figs. 23–25, good solutions are obtained using all methods with a sufficiently small time step. Then as we increase the time step size, the standard Bathe method gives an inaccurate solution first with too large a time step value, and as the time step further increases, a response without the oscillation. The other two methods show, for the selected time steps, less error to the analytical solution but a significant period elongation.

5.2.2. *A double pendulum*

The frictionless double pendulum we consider consists of two point masses m_1 and m_2, connected by rigid weightless rods of length l_1 and l_2, see Fig. 26. The initial conditions are $\theta_1(0) = 0$, $\theta_2(0) = \pi/2$, $\dot{\theta}_1(0) = 0$

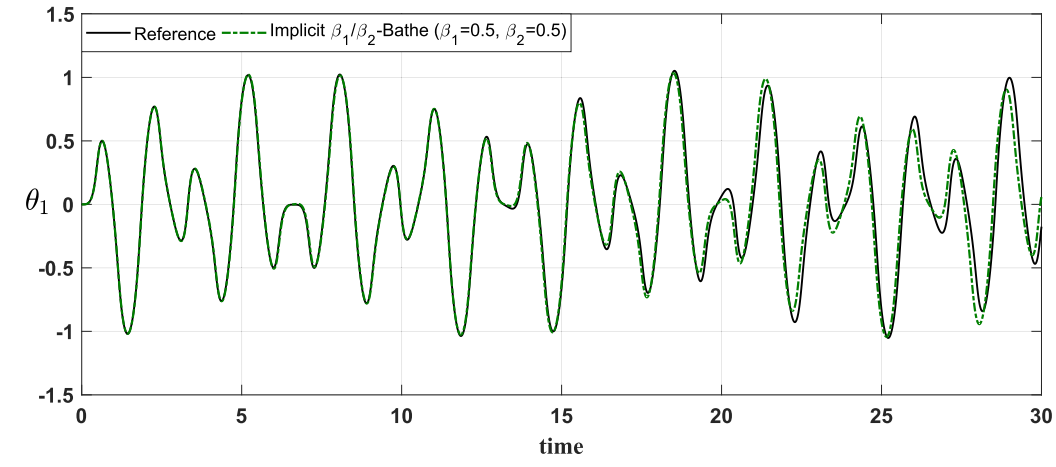

(a) θ_1

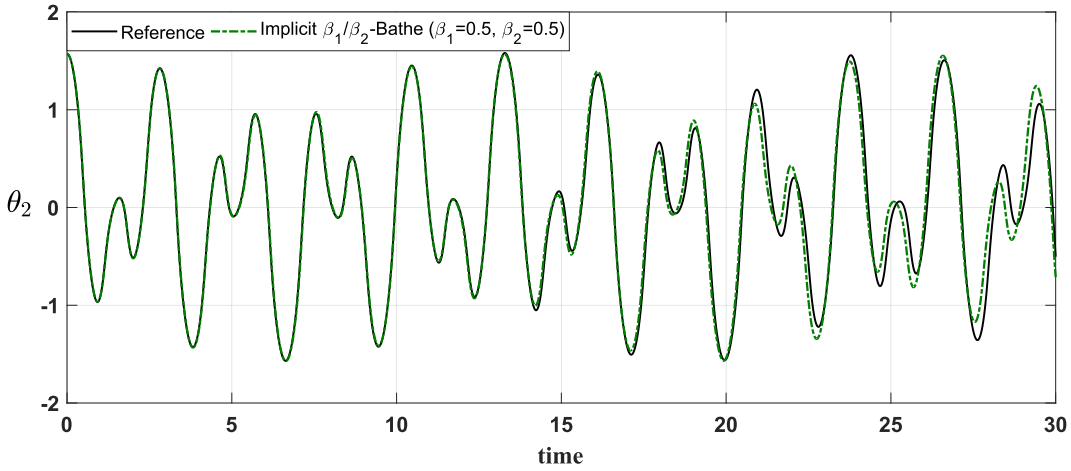

(b) θ_2

Fig. 31. Predicted angular displacements using implicit β_1/β_2-Bathe method with $\Delta t = 0.01$.

and $\dot{\theta}_2(0) = 0$. We solve this example problem with $\Delta t = 0.1$ and $\Delta t = 0.01$. The reference solution has been obtained using the 4th-order explicit Runge-Kutta method with $\Delta t = 0.005$. As shown in Figs. 27–32, when the time step $\Delta t = 0.1$ is used, all response predictions are not accurate, but the implicit β_1/β_2-Bathe scheme gives almost a good solution. When the time step $\Delta t = 0.01$ is used, the response predictions of all three methods are close to the reference solution. Hence, as expected, using a sufficiently small time step we obtain an accurate solution.

6. Concluding remarks

The objective in this paper was to focus on the performance of the explicit β_1/β_2-Bathe method. The method was proposed earlier [1] to be used as a first-order or second-order solution scheme. In the present paper we strived to establish values of the two parameters β_1 and β_2 that yield optimal accuracy, analyzed the method when physical damping is included, and showed the application of the scheme in nonlinear analysis.

To establish a general time integration scheme with parameter values with which always optimal solutions are obtained is almost impossible. The range of different applications in the solution of structural vibrations and wave propagations is too large for that aim to be totally achieved. However, we gave in the paper recommendations for values to use, and showed that with these recommendations, used as a first-order or second-order scheme, good to remarkably accurate results are obtained in the problems solved. In particular, the solutions of long time wave propagations considered in the paper were accurately predicted using the first-order scheme.

While physical damping can directly be included because the damping effect is only part of the effective load vector – which is an advantage of the scheme – we showed in the paper that the critical time step for solutions then decreases. This affects the choice of time step to be used in practice when physical damping is present.

The use of the method in general nonlinear analysis is immediate and only affects how the effective load vector needs to be calculated. We give the governing equations in the paper and show some applications.

We can conclude that the explicit β_1/β_2-Bathe method is a very promising general time integration scheme, but further studies of the method would be valuable. It might be possible to refine the recommendations for use of the method when not considering the scheme for all possible analysis problems (as we did in this paper), but only for particular applications, like for earthquake analysis of buildings. An important field to consider is also the dynamic solution of contact problems, leading to impact and wave propagations which might be solved quite accurately with the scheme. For these special applications it

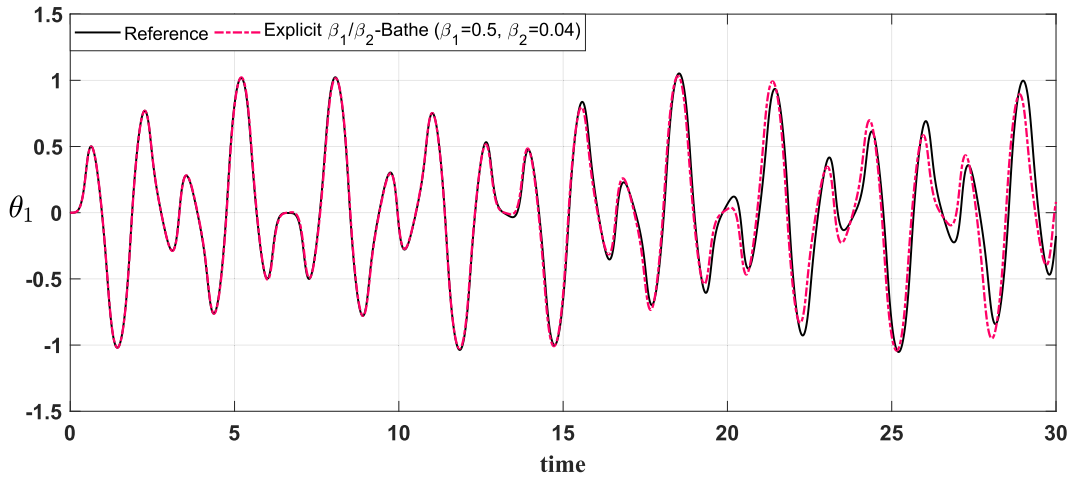

(a) θ_1

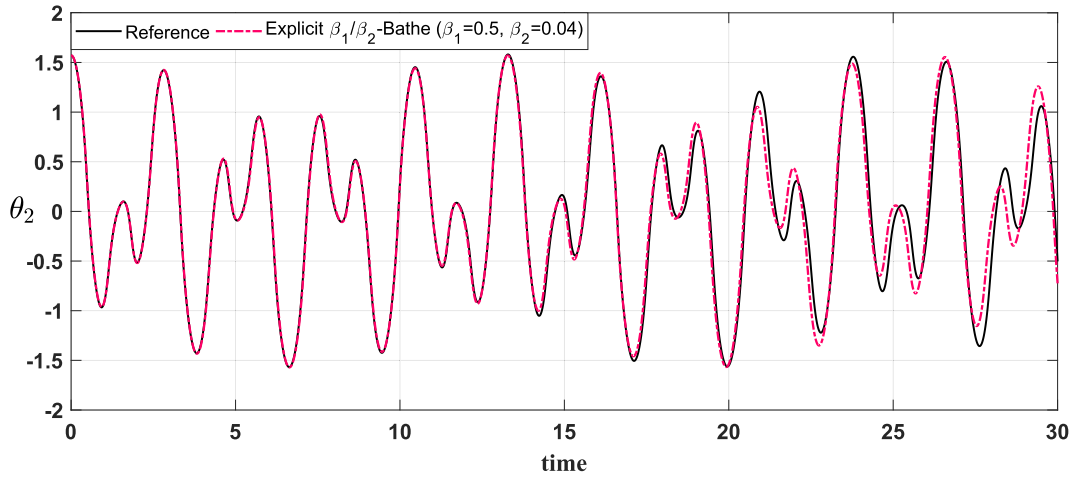

(b) θ_2

Fig. 32. Predicted angular displacements using explicit β_1/β_2-Bathe method with $\Delta t = 0.01$.

would be very valuable to explore the use of machine learning for identifying and using the optimal values of parameters within the two ranges given [34]. The implicit β_1/β_2-Bathe method was already used with overlapping finite elements and the consistent mass matrix to solve wave propagations and performed remarkably well [35]. It would now be very valuable to identify the accuracy of the explicit scheme presented here when used with overlapping finite elements and a lumped mass matrix. Furthermore, the use of the time integration scheme should be explored in the solution of multiphysics problems that increasingly will be tackled in the future.

CRediT authorship contribution statement

Mohammad Mahdi Malakiyeh: Validation, Formal analysis. **Zahra Anjomshoae:** Validation, Formal analysis. **Saeed Shojaee:** Data curation. **Saleh Hamzehei-Javaran:** Formal analysis. **Klaus-Jürgen Bathe:** Writing – review & editing, Validation, Formal analysis.

Declaration of competing interest

The authors declare that they have no known competing financial interests or personal relationships that could have appeared to influence the work reported in this paper.

Data availability

No data was used for the research described in the article.

References

[1] Malakiyeh MM, Shojaee S, Hamzehei-Javaran S, Bathe KJ. The explicit $\beta 1/\beta 2$-Bathe time integration method. Comput Struct 2023;286:107092.
[2] Bathe KJ. Finite element procedures: Prentice Hall; 1996, 2nd edition KJ Bathe, Watertown, MA, 2014; also published by Higher Education Press China 2016.
[3] Dokainish MA, Subbaraj K. A survey of direct time integration methods in computational structural dynamics. I. Explicit methods. Comput Struct 1989;32(6):1371–86.
[4] Subbaraj K, Dokainish MA. A survey of direct time integration methods in computational structural dynamics. II. Implicit methods. Comput Struct 1989;32(6):1387–401.
[5] Newmark NM. A method of computation for structural dynamics. J Eng Mec Div, ASCE 1959;85(3):67–94.
[6] Bathe KJ, Wilson EL. Stability and accuracy analysis of direct integration methods. Int J Earthq Eng Struct Dyn 1973;1(3):283–91.

[7] Chung J, Hulbert GM. A time integration algorithm for structural dynamics with improved numerical dissipation: the generalized-alpha method. J Appl Mech Trans ASME 1993;60:371–5.
[8] Bathe KJ, Baig MMI. On a composite implicit time integration procedure for nonlinear dynamics. Comput Struct 2005;83:2513–24.
[9] Bathe KJ. Conserving energy and momentum in Nonlinear dynamics: a simple implicit time integration scheme. Comput Struct 2007;85:437–45.
[10] Bathe KJ, Noh G. Insight into an implicit time integration scheme for structural dynamics. Comput Struct 2012;98:1–6.
[11] Noh G, Bathe KJ. An explicit time integration scheme for the analysis of wave propagations. Comput Struct 2013;129:178–93.
[12] Liua T, Huanga F, Wen W, He W, Duan S, Fang D. Further insights of a composite implicit time integration scheme and its performance on linear seismic response analysis. Eng Struct 2021;241:112490.
[13] Malakiyeh MM, Shojaee S, Hamzehei-Javaran S. Development of a direct time integration method based on Bezier curve and 5th-order Bernstein basis function. Comput Struct 2018;194:15–31.
[14] Malakiyeh MM, Shojaee S, Hamzehei-Javaran S. Insight into an implicit time integration method based on Bezier curve and third-order Bernstein basis function for structural dynamics. Asian J Civ Eng 2018;19(1):1–11.
[15] Malakiyeh MM, Shojaee S, Hamzehei-Javaran S, Tadayon B. Further insights into time-integration method based on Bernstein polynomials and Bezier curve for structural dynamics. Int J Struct Stab Dyn 2019:1950113.
[16] Malakiyeh MM, Shojaee S, Bathe KJ. The Bathe time integration method revisited for prescribing desired numerical dissipation. Comput Struct 2019;212:289–98.
[17] Malakiyeh MM, Shojaee S, Hamzehei-Javaran S, Bathe KJ. New insights into the $\beta 1/\beta 2$-Bathe time integration scheme when L-stable. Comput Struct 2021;245:106433.
[18] Soares D. A novel family of explicit time marching techniques for structural dynamics and wave propagation models. Comput Methods Appl Mech Eng 2016;311:838–55.
[19] Soares D. A novel time-marching formulation for wave propagation analysis: the adaptive hybrid explicit method. Comput Methods Appl Mech Eng 2020;366:113095.
[20] Wood WL. Practical time-stepping schemes. Oxford: Clarendon Press; 1990.
[21] Chung J, Lee JM. A new family of explicit time integration methods for linear and non-linear structural dynamics. Int J Numer Methods Eng 1994;37:3961–76.
[22] Hulbert GM, Chung J. Explicit time integration algorithms for structural dynamics with optimal numerical dissipation. Comput Methods Appl Mech Eng 1996;137:175–88.
[23] Chang SY, Liao WI. An unconditionally stable explicit method for structural dynamics. J Earthq Eng 2005;9:349–70.
[24] Noh G, Ham S, Bathe KJ. Performance of an implicit time integration scheme in the analysis of wave propagations. Comput Struct 2013;123:93–105.
[25] Benitez JM, Montans FJ. The value of numerical amplification matrices in time integration methods. Comput Struct 2013;128:243–50.
[26] Noh G, Bathe KJ. Imposing displacements in implicit direct time integration & a patch test. Adv Eng Softw Comput Struct 2023;175:103286.
[27] Wood WL. Numerical integration of structural dynamics equations including natural damping and periodic forcing terms. Int J Numer Methods Eng 1981;17(2):281–9.
[28] Wood WL. A unified set of single step algorithms. Part 2: theory. Int J Numer Methods Eng 1984;20(12):2303–9.
[29] Depouhon A, Detournay E, Denoël V. Accuracy of one-step integration schemes for damped/forced linear structural dynamics. Int J Numer Methods Eng 2014;99(5):333–53.
[30] Kim W, Choi SY. An improved implicit time integration algorithm: the generalized composite time integration algorithm. Comput Struct 2018;196:341–54.
[31] Kim W, Reddy JN. A new family of higher-order time integration algorithms for the analysis of structural dynamics. J Appl Mech 2017;84(7):071008.
[32] Kim W, Lee JH. An improved explicit time integration method for linear and nonlinear structural dynamics. Comput Struct 2018;206:42–53.
[33] D'Alessio S. An analytical, numerical and experimental study of the double pendulum. Eur Phys Soc 2023;44:015002.
[34] Rabczuk T, Bathe KJ, editors. Machine learning in modeling and simulation. Springer; 2023.
[35] Kim KT, Bathe KJ. Accurate solution of wave propagation problems. Comput Struct 2021;249:106502.